Charge-Transfer Interactions in Face-to-Face Porphyrin–Fullerene Systems: Solvent-Dependent Luminescence in the Infrared Spectral Region

Nicola Armaroli,*[a] Giancarlo Marconi,[a] Luis Echegoyen,*[b] Jean-Pascal Bourgeois,[c] and François Diederich*[c]

Abstract: The cyclophane-type molecular dyads **1·2H** and **1·Zn**, in which a doubly bridged porphyrin donor adopts a close, tangential orientation relative to the surface of a fullerene acceptor, were prepared by Bingel macrocylization. The porphyrin derivatives **2·2H** and **2·Zn** with two appended, singly linked C_{60} moieties were also formed as side products. NMR investigations revealed that the latter compounds strongly prefer conformations with one of the carbon spheres nesting on the porphyrin surface, thereby taking a similar orientation to that of the fullerene moiety in the doubly bridged systems. Cyclic voltammetric measurements showed that the mutual electronic effects exerted by the fullerene on the porphyrin and vice versa are only small in all four dyads, despite the close proximity of the donor and acceptor components. The steady-state and time-resolved absorption and luminescence properties of **1·Zn** and **2·Zn** were investigated in toluene solution and it was shown that, upon light excitation, both the porphyrin- and the fullerene-centered excited states are deactivated to a lower-lying CT state, emitting in the IR spectral region ($\lambda_{max} = 890$ and 800 nm at 298 and 77 K, respectively). In the more polar solvent benzonitrile, this CT state is still detected but, owing to its very low energy (below 1.4 eV), is not luminescent and shorter-lived than in toluene. The remarkable observation of similar photophysical behavior of **1·Zn** and **2·Zn** suggests that a tight donor–acceptor distance cannot only be established in doubly bridged cyclophane-type structures but also in singly bridged dyads, by taking advantage of favourable fullerene–porphyrin ground-state interactions.

Keywords: charge transfer · dyads · fullerene · IR luminescence · porphyrin

Introduction

Molecular dyads composed of an energy or electron donor capable of photoinduced energy- or electron-transfer to a covalently linked acceptor component have been widely studied as mimics of the natural photosynthetic reaction centers and as photochemical molecular devices.[1] It is not too surprising that C_{60}, with its demonstrated strong electron-accepting capability, has been widely introduced into molecular dyads,[2, 3] once the covalent chemistry of the carbon sphere was developed.[4] In particular, a variety of systems containing a porphyrin as electron donor and C_{60} as electron acceptor have been constructed in recent years.[5] In these compounds, the porphyrin usually is attached to the fullerene by a single linker and, consequently, distance and orientation between the two components are often not well defined. For an enhanced control of these essential geometrical parameters, we applied our tether-directed remote functionalization strategy[6] and attached the porphyrin to two points of the C_{60} surface leading to the formation of a cyclophane structure.[7, 8] Here, we report the synthesis of the porphyrin–C_{60} conjugates **1·2H** and **1·Zn**, with a *trans*-1 addition pattern on the carbon sphere, by regioselective Bingel macrocyclization.[6a–c, 9] This reaction afforded as interesting by-products conjugates **2·2H** and **2·Zn**, with two fullerenes attached via single linkers to one porphyrin (Figure 1). The extent of interchromophoric interactions in the ground state of these four compounds is analyzed electrochemically by cyclic voltammetry (CV). The photophysical behavior of the zinc complexes **1·Zn** and **2·Zn** is comprehensively studied in comparison to model porphyrin **3·Zn** and two fullerene derivatives, *trans*-1 bis-adduct **4**,[10] and mono-adduct **5**.[11]

[a] Dr. N. Armaroli, Dr. G. Marconi
Istituto di Fotochimica e Radiazioni d'Alta Energia del CNR
Via Gobetti 101, 40129 Bologna (Italy)
Fax: (+39) 051 639 9844
E-mail: armaroli@frae.bo.cnr.it

[b] Prof. Dr. L. Echegoyen
Department of Chemistry, University of Miami
Coral Gables, FL 33124 (USA)
Fax: (+1) 305 284-4571
E-mail: echegoyen@miami.edu

[c] Dipl.-Chem. J.-P. Bourgeois, Prof. Dr. F. Diederich
Laboratorium für Organische Chemie, Universitätstrasse 16
8092 Zürich (Switzerland)
Fax: (+41) 1 632 1109
E-mail: diederich@org.chem.ethz.ch

  0947-6539/00/0609-1629 $ 17.50+.50/0

These investigations provide evidence for a remarkable similarity in the photophysical behavior of the singly (**2·Zn**) and doubly (**1·Zn**) bridged Zn^{II} porphyrin–fullerene conjugates. In both systems, strong interchromophoric interactions give rise to a low-lying CT state which emits in the near infrared region.

Results

Synthesis: The porphyrin-tethered bis(malonates) **3·2H/3·Zn** were designed with the help of molecular modeling[12] to ensure formation of a *trans*-1 addition pattern during Bingel macrocyclization with C_{60}. Starting from aldehyde **6**,[13] compound **3·2H** was obtained by two routes. In the first one, esterification of **6** afforded malonate **7** which was cyclized with dipyrromethane **8** in the presence of CF_3COOH (TFA) to yield, after oxidation with chloranil, the bis-malonate-appended porphyrin in 5% yield (Scheme 1).[14] The low yield of **3·2H** is due to the reversibility of porphyrinogen formation[14] which leads to a mixture of porphyrins containing four, three, two (**3·2H** and a regioisomer), one, and zero malonate-appended *meso*-phenyl rings, respectively. Furthermore, separation of **3·2H** from its regioisomer, with adjacent malonate-appended *meso*-phenyl rings, proved to be quite challenging, in view of almost identical compound polarity, and required multiple chromatography on SiO_2-*H*. The identity of **3·2H** was confirmed by the ^{13}C-NMR spectrum (125.8 MHz, $(CDCl_2)_2$, 380 K) which showed the expected 18 sp^2-C-atom resonances; a total of 22 such resonances would be expected in the spectrum of the other regioisomer. The second route to **3·2H** involved the simple mixing of benzaldehyde (1 equiv), 3-hydroxymethylbenzalhyde (**6**) (1 equiv), and pyrrole (2 equiv), reversible porphyrinogen formation with TFA,[14] and oxidation with 2,3-dichloro-5,6-dicyano-1,4-benzoquinone (DDQ) to give **9** in 3% yield. Although the yield was poor again, separation of **9** from its regioisomer, with significantly different polarity, proceeded much more smoothly by a single column chromatography on SiO_2. Diol **9** was subsequently transformed in 80% yield into bis-malonate **3·2H**.

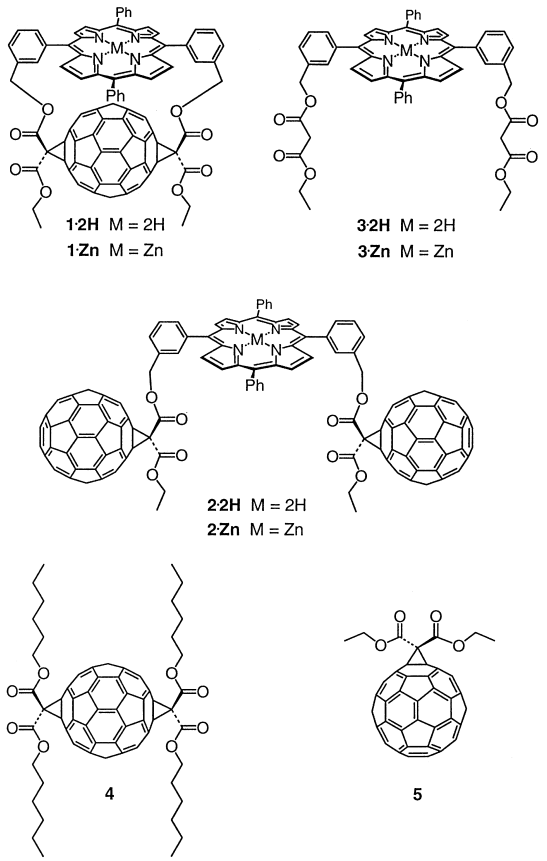

Figure 1. Compounds subjected to electrochemical and photophysical investigations in this study.

The modified Bingel reaction of **3·2H** with C_{60} in toluene provided, after chromatography, the desired *trans*-1 bis-adduct **1·2H** in 17% yield together with <2% of the bis-fullerene appended porphyrin **2·2H**, and a third fraction of non-characterized compounds (8%). The regioselectivity in the macrocyclization reaction is quite high; other regioisomers were only produced in minor amounts and could not be isolated in pure form. Compound **2·2H** can also be obtained as the major product when an excess of C_{60} is used in the Bingel reaction: with 5 equivalents C_{60} at 0°C, **2·2H** was

Abstract in Italian: *Le diadi molecolari ciclofaniche **1·2H** e **1·Zn**, ove una porfirina elettron-donatrice viene a trovarsi vicina, e in posizione tangenziale, rispetto alla superficie di un fullerene elettro-accettore, sono state preparate mediante reazione di macrociclizzazione di Bingel. Come prodotti secondari di reazione sono stati ottenuti i derivati porfirinici **2·2H** and **2·Zn**, che presentano alle estremità due unità fullereniche appese di tipo monosostituito. Gli studi NMR evidenziano che in questi ultimi è favorita una conformazione in cui una sfera fullerenica si posiziona in stretta vicinanza alla superficie della porfirina, analogamente a quanto accade per le diadi ciclofaniche **1·2H** e **1·Zn**. Misure di voltammetria ciclica indicano che la mutua interazione tra il fullerene e la porfirina sono modeste in tutti e quattro i casi, nonostante la stretta vicinanza dei componenti e le loro complementari proprietà elettroniche. Le proprietà di assorbimento ed emissione di **1·Zn** e **2·Zn**, sia allo stato stazionario che risolte nel tempo, sono state studiate in toluene. E' stato così dimostrato che, a seguito di assorbimento di luce, sia gli stati eccitati localizzati sulla porfirina che quelli localizzati sul fullerene vengono disattivati verso un più basso livello elettronico di trasferimento di carica (CT), che emette nel vicino infrarosso (λ_{max} = 890 e 800 nm a 298 e 77 K, rispettivamente). In un solvente più polare, quale benzonitrile, lo stato CT è ancora osservato ma, a causa del basso contenuto energetico (meno di 1.4 eV), non è luminescente e presenta un tempo di vita più breve che in toluene. Risulta di particolare rilevanza la somiglianza tra il comportamento fotofisico di **1·Zn** e **2·Zn**; questo suggerisce che una stretta vicinanza tra il donatore e l'accettore può realizzarsi non solo nelle strutture forzatamente affacciate di tipo ciclofanico, ma anche nei sistemi "non costretti" con due unità fullereniche, sfruttando favorevoli interazioni donatore-accettore allo stato fondamentale.*

  0947-6539/00/0609-1630 $ 17.50+.50/0 *Chem. Eur. J.* **2000**, *6*, No. 9

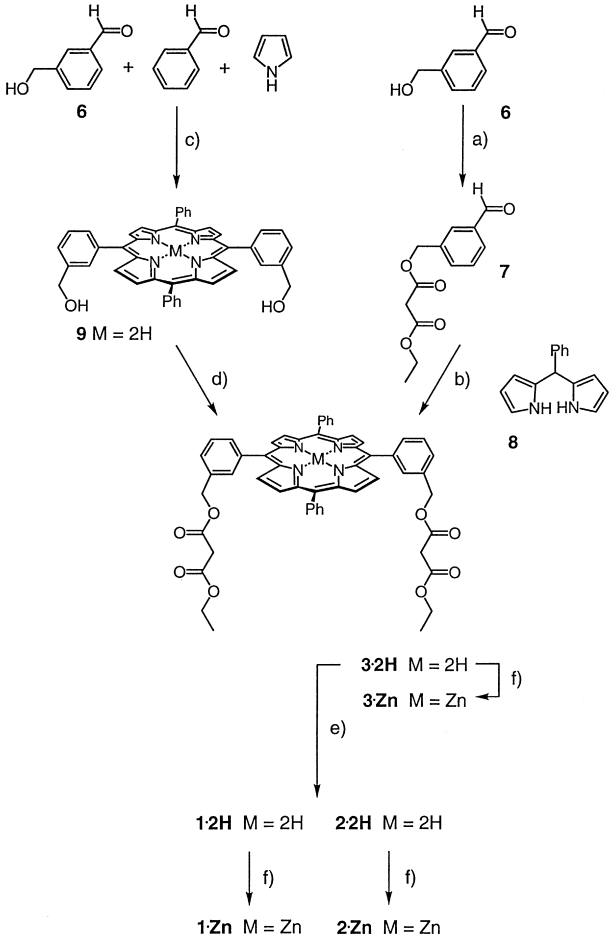

Scheme 1. Synthesis of **1·Zn** and **2·Zn**. a) $ClCOCH_2CO_2Et$, Et_3N, CH_2Cl_2, 20 °C, 1 h, 87 %; b) TFA, CH_2Cl_2, 20 °C, 24 h, then chloranil, 20 °C, 1 h, 5 %; c) TFA, CH_2Cl_2, 20 °C, 24 h, then DDQ, 20 °C, 1 h, 3 %; d) $ClCOCH_2CO_2Et$, Et_3N, CH_2Cl_2, 20 °C, 1 h; 80 %; e) C_{60}, I_2, 1,8-diazabicyclo[5.4.0]undec-7-ene (DBU), toluene, 20 °C, 1 h, 17 % (**1·2H**), < 2 % (**2·2H**); f) $Zn(OAc)_2$, $CHCl_3$/MeOH 1:1, 20 °C, 1 h, quantitative yield.

obtained in 44 % yield (with respect to starting material **3·2H**). Quantitative metallation with $Zn(OAc)_2$ afforded **1·Zn**, **2·Zn**, and **3·Zn**, respectively. Bingel macrocylization of zinc derivative **3·Zn** with C_{60} did not provide any advantages in yield or regioselectivity as compared with the described reaction of **3·2H**.

The relative position of the two cyclopropyl groups on the C_{60} surface in **1·2H** and **1·Zn** was unambiguously established by ^{1}H- and ^{13}C-NMR spectroscopy, which clearly demonstrated the C_{2v} symmetry of the two dyads. In the ^{1}H-NMR spectrum (500 MHz, $CDCl_3$) of both compounds, the PhCH_2O protons appeared as a sharp singlet. Their ^{13}C-NMR spectra (125.8 MHz, $CDCl_3$) displayed the expected five sp^3-C-atom resonances besides 34 sp^2-C-atom resonances for the fullerene and tetraphenylporphyrin moieties and the malonate C=O groups. Among all possible regioisomeric macrocyclic dyads, a symmetry as high as C_{2v} can only be present if the addition pattern on the fullerene surface is *trans*-1 with an *out*–*out* orientation of the two ethoxycarbonyl groups.

Matrix-assisted laser-desorption-ionization time-of-flight (MALDI-TOF) and fast-atom bombardment (FAB) spectra of **2·2H** and **2·Zn** were in full agreement with the proposed structures featuring two C_{60} spheres appended to one porphyrin ring. However, the number and multiplicity of the resonances in the ^{1}H- and ^{13}C-NMR spectra at 298 K did not reflect the initially assumed C_{2v}-symmetry of these two compounds, but rather a time-averaged C_s-geometry with a distinct set of resonances for each of the two fullerene-malonate side arms. Comparable resonances in each of the two sets appear with equal intensity. This also holds for the spectra recorded at 380 K, although strong broadening of the resonances starts appearing at the higher temperature. The ^{1}H-NMR spectra (298 K) of **2·2H** and **2·Zn** display two singlets for two PhCH_2O methylene groups and two sets of a triplet and a quadruplet for the two CH_3CH_2O groups. The ^{13}C-NMR (125.8 MHz, $(CDCl_2)_2$, 298 K) spectrum of **2·2H** shows ten resonances for sp^3-C atoms, as expected for C_s-symmetry, and 72 out of the 93 expected resonances for sp^2-C atoms. The spectrum of **2·Zn** features all 93 expected sp^2-C-atom resonances. These NMR data are best explained by assuming a slow equilibration between two degenerate, C_s-symmetrical conformers with one fullerene component oriented below the plane of the porphyrin and the other one pointing away (Figure 2). The two carbon spheres can be located on the same or on opposite sides of the porphyrin ring; however, this is not observable experimentally since the atropisomerization mechanism, which exchanges the side on which the outward pointing fullerene is located, is fast on the NMR time scale.

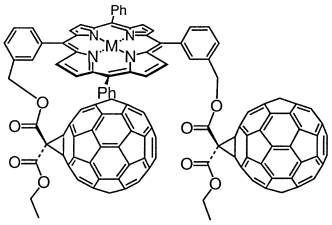

Figure 2. Preferred conformation of **2·2H** (M = 2H) and **2·Zn** (M = Zn) according to ^{1}H- and ^{13}C-NMR spectroscopy.

Dihedral angle preferences in the side chains connecting the fullerene moieties to the porphyrin could possibly account for the geometrical preferences adopted by **2·2H** and **2·Zn**. Also, a time-averaged geometry as schematically proposed in Figure 2, with both carbon spheres in spatial proximity, could benefit from attractive fullerene – fullerene contacts. We believe, however, that attractive porphyrin – fullerene interactions[15] are mainly responsible for the preference of **2·2H** and **2·Zn** for C_s-symmetrical conformations in which one fullerene adopts an orientation with respect to the porphyrin which is similar to that of the doubly bridged carbon sphere in the *trans*-1 bis-adducts **1·2H** or **1·Zn**. This conformational preference is further supported by the photophysical studies described below. Interestingly, the C_{2h}-symmetrical conformation, with the two fullerenes sandwiching the porphyrin moiety is not observed; this could be taken as an indication that the two fullerenes prefer being located on one side of the porphyrin macrocycle where they can have attractive contacts with one another.

Electrochemistry: In the electrochemical studies, *trans*-1 bis-adduct **4** and mono-adduct **5** were used as models to assess the electronic effects, if any, of the porphyrin on the measured reduction potentials (cathodic processes) of the fullerene component in conjugates **1·2H/1·Zn** and **2·2H/2·Zn**. Compounds **3·2H** and **3·Zn** are good models to evaluate the effects of the fullerene moieties on the porphyrin-based oxidation potentials (anodic processes) in the conjugates. The results of the cyclic voltammetric studies are summarized in Table 1.

Table 1. Redox potentials in Ar-degassed CH_2Cl_2 and benzonitrile containing 0.1M Bu_4NPF_6 as supporting electrolyte.

Compound	Reduction			Oxidation	
	$E^1_{1/2}$	$E^2_{1/2}$	$E^3_{1/2}$	$E^1_{1/2}$	$E^2_{1/2}$
1·2H	−1.11 (70)[a]	−1.54 (90)	–	0.57 (60)	0.94 (70)
2·2H	−1.05 (84)[b]	−1.39 (91)[b]	−1.62 (66)	0.58 (60)	–
3·2H	−1.67 (82)	−1.97 (120)	–	0.55 (75)	0.87 (80)
4	−1.09 (76)	−1.47 (79)	–	–	–
	−0.98 (90)[c]	−1.43 (100)[c]	–	–	–
5	−0.96 (76)[c]	−1.38 (98)[c]	–	–	–
1·Zn	−1.13 (71)	−1.54 (90)	–	0.38 (74)	0.71 (75)
	−1.05 (80)[c]	−1.51 (−)[c]	–	0.33 (90)[c]	–
2·Zn	−1.09 (71)[b]	−1.45 (103)[b]	–	0.72 (54)	0.37 (62)
	−0.97 (94)[b,c]	−1.36 (106)[b,c]	–	–	0.36 (76)[c]
3·Zn	−1.83 (73)	–	–	0.37 (72)	0.67 (78)
	−1.83 (−)[c]	–	–	0.35 (110)[c]	–

[a] Values in parenthesis are the ΔE_{pp} in mV. [b] Two-electron reduction steps. [c] Measured in dry benzonitrile.

In general and somewhat unexpectedly, while some differences were observed, it can be stated that the changes in potential of one component due to the presence of the other one, were typically small. For example, comparing the first reduction potential of **4** with that of **1·2H** shows only a 20 mV cathodic shift, while the effect on the second reduction is somewhat larger at 70 mV. These reductions are all fullerene-based, as confirmed by the results obtained for **2·2H** and **2·Zn**, which clearly show that these peaks are twice as large as those corresponding to the oxidation of the porphyrin moiety.[7] Interestingly, the first reduction process for **3·2H** (−1.67 V) occurs at a potential that is very close to the second reduction step for **1·2H** (−1.54 V), which is C_{60}-centered.

Anodic scans revealed even smaller effects of the fullerene moiety on the oxidation potentials of the porphyrin chromophore. For example, bis-malonate-appended porphyrin **3·2H** has a first oxidation potential of 0.55 V, while the corresponding process for **1·2H** occurs at 0.57 V. An electronic effect of the fullerene is more pronounced for the second porphyrin-centered oxidation process, which occurs at 0.87 V for **3·2H** but at 0.94 V for **1·2H**, corresponding to a 70 mV shift.

While the introduction of the Zn^{II} ion caused pronounced potential shifts (between 160 and 200 mV cathodic shifts of both oxidation and reduction processes when changing from **3·2H** to **3·Zn**), it had almost no effect on the fullerene-based reductions in the cyclophane dyad. Thus, **1·Zn** has a fullerene-based first reduction potential of −1.13 V, which is very close to the corresponding value measured for **1·2H** (−1.11 V), and the second, fullerene-based reduction process occurs exactly at the same potential (−1.54 V) in both compounds.

Electrochemical measurements in benzonitrile show a general anodic shift of the fullerene-centered reduction potentials since the polar solvent stabilizes the charged species more effectively than CH_2Cl_2. The second porphyrin-based oxidation is not observed since the solvent potential window precludes it. Otherwise, the compounds show very similar behavior in both solvents. Therefore, in general, it can be stated that the mutual electronic effects exerted by the fullerene on the porphyrin and vice versa in dyads **1·2H** and **1·Zn** are relatively small and thus any ground-state donor–acceptor interactions are hardly measurable by electrochemistry.

Photophysics

Steady-state absorption spectra: The electronic absorption spectra of the reference compounds **3·Zn**, **4**, and **5** in toluene solution are shown in Figure 3. In the UV region, the fullerene absorption is stronger than that of the porphyrin, whereas in the visible spectral region an opposite pattern is observed. The spectrum of **3·Zn** is quite similar to that of Zn^{II} tetra(*meso*-phenyl)porphyrin (ZnTPP).[16] The maximum of the Soret band, corresponding to the transition to the second singlet excited state, is located at 422 nm (ε = 453000 M^{-1} cm^{-1}). The two reference fullerenes display rather different spectral shapes in the visible spectral region whereas in the UV they bear great similarity.

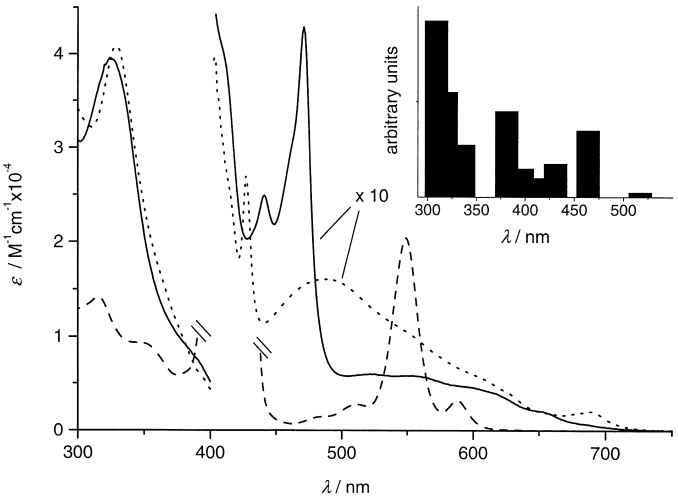

Figure 3. Absorption spectra of **3·Zn** (dashed line), **4** (full line), and **5** (dotted line) in toluene solution at 298 K. For **4** and **5**, the 400–750 nm portion of the spectrum is multiplied ten times; for **3·Zn**, the Soret band portion around 425 nm is truncated for the sake of clarity. Inset: spectrum of **4** from theoretical calculations, reporting electronic transitions only.

Interestingly, the spectrum of **4** exhibits two sharp and intense maxima at 441 and 471 nm with molar absorption coefficients of 2500 and 4300 M^{-1} cm^{-1}, respectively, mainly responsible for the characteristic deep-yellow color of this compound in solution. Above 500 nm, the spectrum of **4** is less intense than that of **5** and presents a series of contiguous shoulders. Compound **5** shows one sharp and intense band at

0947-6539/00/0609-1632 $ 17.50+.50/0 *Chem. Eur. J.* **2000**, *6*, No. 9

428 nm ($\varepsilon = 2700\,\text{M}^{-1}\,\text{cm}^{-1}$), and an additional weak maximum is detected at 683 nm ($\varepsilon = 200\,\text{M}^{-1}\,\text{cm}^{-1}$). The appearance of both bands is highly characteristic for fullerene monoadducts.[17]

The absorption spectra of the fullerene – porphyrin conjugates **1 · Zn** and **2 · Zn** are reported in Figures 4 and 5, along with the shapes obtained by simply adding the spectra of the pertinent component units.

In both cases, experimental and mathematical spectra display good superimposition in the UV region, whereas in the Vis region strong differences are observed. In particular, a red-shift ($\lambda_{max} = 428$ and 426 nm for **1 · Zn** and **2 · Zn**, respectively) and strong intensity decrease of the Soret bands is evident, whereas the Q-bands are less affected. A weak tail up to 800 nm is observed in toluene solution, even further extending into the near-IR (NIR) in benzonitrile (Figures 4 and 5, inset).

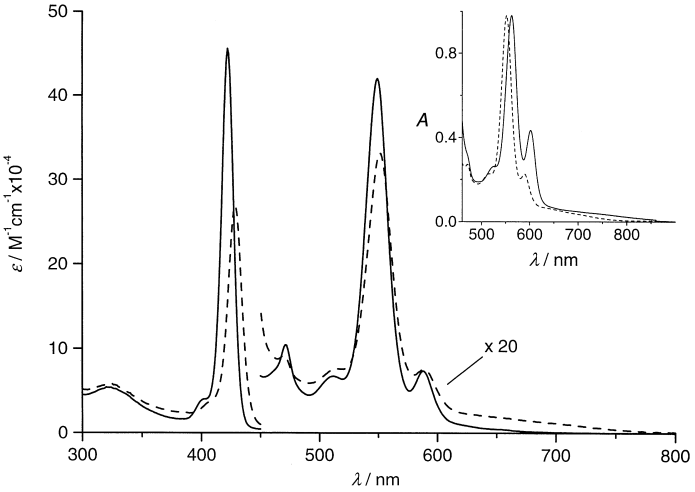

Figure 4. Comparison between the absorption spectrum of **1 · Zn** (dashed line) and that obtained from the sum of its components **3 · Zn** and **4** (full line) in toluene solution at 298 K. The 450 – 800 nm portion of the spectrum is multiplied 20 times. Inset: absorption spectrum of **1 · Zn** in toluene (dashed line) and benzonitrile (full line), normalized on the Q-bands maxima.

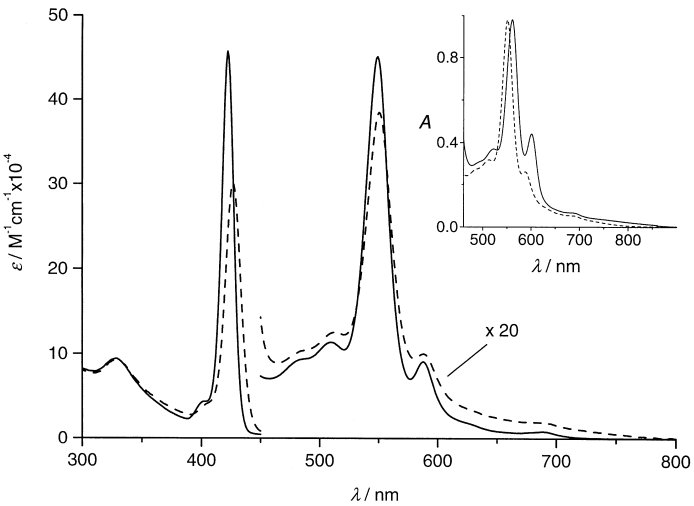

Figure 5. Comparison between the absorption spectrum of **2 · Zn** (dashed line) and that obtained from the sum of its components **3 · Zn** and **4** (full line) in toluene solution at 298 K. The 450 – 800 nm portion of the spectrum is multiplied 20 times. Inset: absorption spectrum of **2 · Zn** in toluene (dashed line) and benzonitrile (full line), normalized on the Q-bands maxima.

Luminescence spectra and lifetimes: The most relevant luminescence data for all the investigated compounds are reported in Table 2, where the luminescence band maxima refer to spectra uncorrected for detector response.

In toluene solution at room temperature, **3 · Zn** exhibits a fluorescence band ($\lambda_{max} = 644$ nm, $\tau = 1.9$ ns, $\Phi_{em} = 0.013$, Figure 6), whereas at 77 K both fluorescence ($\lambda_{max} = 596$ nm,

Table 2. Luminescence and transient absorption data in toluene.

	Luminescence					Transient absorption, 298 K			
	298 K			77 K		$S_1 \rightarrow S_n$ or CT		$T_1 \rightarrow T_n$	
	λ_{max}[a] (nm)	τ[b] (ps)	Φ_{em} ($\times 10^{-4}$)	λ_{max} (nm)	τ[c] (ns)	λ_{max} (nm)	τ (ps)	λ_{max} (nm)	τ (μs)
4	766	1600	2	804	2.2	520, 710	1500	695	0.260[d] 30[e]
5	700	1700	5	694	2.0	535, 750, 900	1600	710	0.280[d] 23[e]
3 · Zn	644	1900	130	596[f] 778[g]	3.1 2.5×10^7	490, 575, 610, 680	2000	470	0.560[d] 130[e]
1 · Zn	800[h] 926[i]	1460 [j]	[k]	750[l]	9.5	480, 620	730	695	0.300[d] 11[e]
2 · Zn	700[h] 926[i]	1400 730	[k]	740[m]	4.2, 62.5[n]	480, 620	720	710	0.280[d] 2.6[e]

[a] From uncorrected emission spectra. [b] From streak camera or time correlated single photon counting (TCSPC) apparatus. [c] From TCSPC apparatus. [d] Air-equilibrated solutions. [e] Oxygen-free solutions. [f] Fluorescence band. [g] Phosphorescence band. [h] Fullerene-localized emission band overlapped with the charge-transfer infrared band. [i] Charge-transfer emission band, corrected value, 890 nm. [j] Impossible to evaluate with the streak camera apparatus, owing to the marked spectral overlap with the fullerene-localized emission. [k] Impossible to evaluate owing to the spectral overlap with the fullerene-localized emission and the lack of reliable standard reference fluorophores in this spectral region. [l] Corrected value, 800 nm. [m] Corrected value, 810 nm. [n] Double exponential decay, the relative amplitude of the two components is equal within the experimental errors.

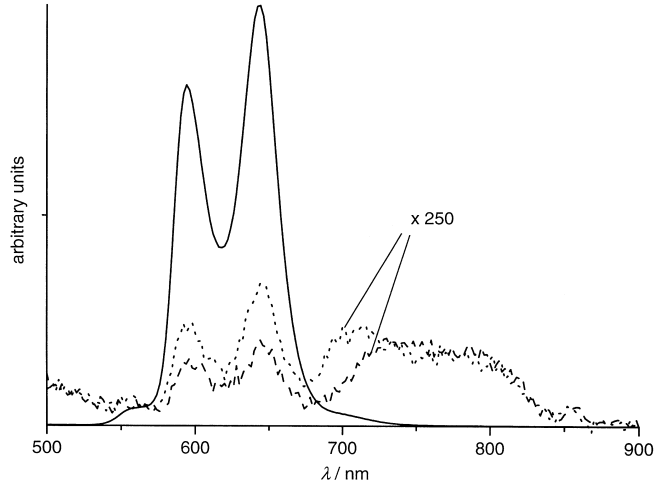

Figure 6. Fluorescence spectra of **3·Zn** (full line), **1·Zn** (dashed line), and **2·Zn** (dotted line) in toluene solution at 298 K; the excitation wavelength is at the maximum of each Soret band, that is at 422.4, 428.2, 426.6 nm, where all samples display $A = 0.350$. The spectra of **1·Zn** and **2·Zn** are multiplied 250 times.

$\tau = 3.1$ ns) and phosphorescence ($\lambda_{max} = 778$ nm, $\tau = 25$ ms) are observed, Figure 7. The porphyrin fluorescence is dramatically quenched (over 500 times) in **1·Zn** and **2·Zn** (Figure 6), whatever the excitation wavelength.

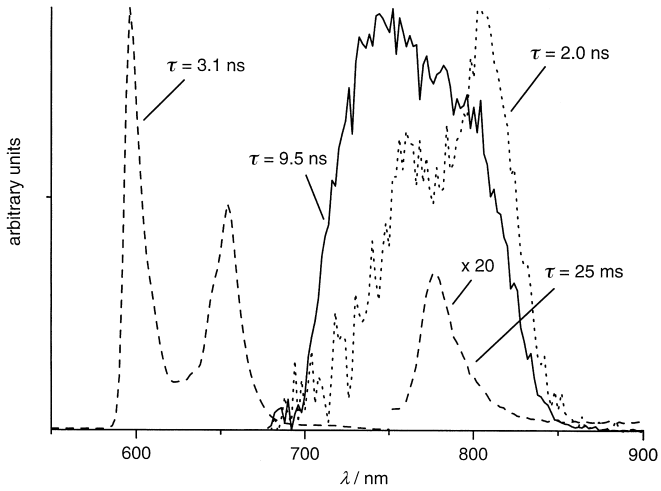

Figure 7. Normalized uncorrected emission spectra of **3·Zn** (dashed line), **4** (dotted line), and **1·Zn** (full line) in a solid toluene matrix at 77 K, upon excitation at 350 nm. The background signal of the toluene matrix has been subtracted, the very weak spectrum of **4** was obtained with a red-enhanced photomultiplier tube. For **3·Zn**, both the fluorescence ($\lambda_{max} = 596$ and 654 nm) and phosphorescence features ($\lambda_{max} = 778$ nm) are observed. In benzonitrile matrix, **1·Zn** (and **2·Zn**) does not show luminescence, unlike all the reference compounds which show spectra similar to those in toluene.

In a time-resolved experiment with a streak camera (picosecond time scale, $\lambda_{exc} = 532$ nm) no trace of a short-living component attributable to the porphyrin fluorescence is observed for **1·Zn**, whereas a very short-living component rising and decaying within the laser pulse duration (35 ps) can be detected for **2·Zn**. In both cases, a faint signal with $\tau =$ 1.9 ns is found, attributable to tiny amounts of **3·Zn** impurities.

In toluene solution at room temperature, a fluorescence band is observed for both the reference fullerene compounds **4** ($\lambda_{max} = 813$ nm, $\tau = 1.6$ ns, $\Phi_{em} = 0.0002$) and **5** ($\lambda_{max} =$ 702 nm, $\tau = 1.7$ ns, $\Phi_{em} = 0.0005$), Figures 8 and 9. Such emission maxima refer to luminescence spectra corrected for the instrumental response (insets of Figures 8 and 9) and, especially for **4** were the correction is dramatic, they are subject to large experimental uncertainty (see Experimental Section).

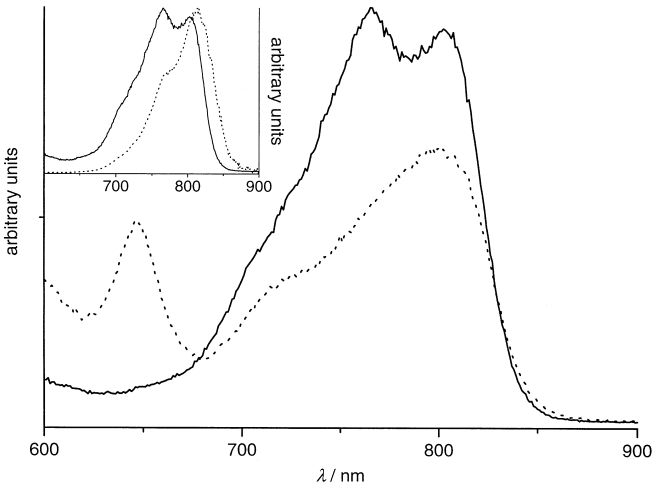

Figure 8. Fluorescence spectra of **4** (full line) and **1·Zn** (dashed line) in toluene solution at 298 K, upon excitation at 325 nm ($A = 0.425$) where, for **1·Zn**, most of the light ($\geq 75\%$) is absorbed by the fullerene moiety. Inset: fluorescence spectrum of **4** uncorrected (full line) and corrected (dotted line) for the photomultiplier response.

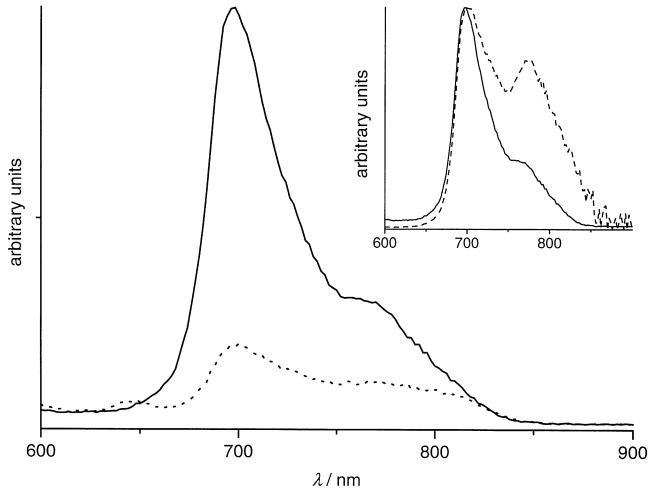

Figure 9. Fluorescence spectra of **5** (full line) and **2·Zn** (dotted line) in toluene solution at 298 K, upon excitation at 330 nm ($A = 0.420$) where, for **2·Zn**, most of the light ($\geq 90\%$) is absorbed by the fullerene fragments. Inset: fluorescence spectrum of **5** uncorrected (full line) and corrected (dashed line) for the photomultiplier response.

Also in rigid matrix at 77 K, both fullerene model compounds exhibit fluorescence with $\lambda_{max} = 804$ nm and $\tau =$ 2.2 ns for **4** (Figure 7) and $\lambda_{max} = 694$ nm and $\tau = 2.0$ ns for **5**. No phosphorescence could be detected under these conditions.

Either upon selective excitation (Soret bands) of the porphyrin moiety (Figure 6) or upon preferential excitation

  0947-6539/00/0609-1634 $ 17.50+.50/0 *Chem. Eur. J.* **2000**, *6*, No. 9

(UV region) of the fullerene fragment (Figures 8 and 9), broad emission bands are found in the 700 – 850 nm spectral region for **1·Zn** and **2·Zn**. Such bands are less intense and appear to be less resolved than those of the corresponding fullerene reference compounds under the same conditions (Figures 8 and 9). The excitation spectra of **3·Zn**, **1·Zn**, and **2·Zn** recorded at $\lambda_{em} = 805$ nm show the characteristic bands of the porphyrin fragment, namely the Soret and Q-bands, the former being exactly located in its peculiar diagnostic position (422, 428, and 426 nm, respectively, see above).

The occurrence of emission bands spanning up to the limit of spectral detection of a conventional UV/Vis spectrofluorimeter prompted us to investigate the luminescence behavior in the IR spectral region (800 – 1350 nm). Some of the spectra obtained (corrected for the germanium detector response) are reported in Figure 10. In this region, the spectrum of the reference compound **4** in toluene starts at its maximum (vide supra), then the IR tail is observed, also accompanied by the sensitized singlet-oxygen luminescence at 1270 nm. On the contrary, **1·Zn** and **2·Zn** exhibit more intense and broader bands with maxima around 890 nm and only weak sensitized singlet-oxygen luminescence. Interestingly, the spectrum of **1·Zn** is wider than that of **2·Zn** towards the Vis spectral side.

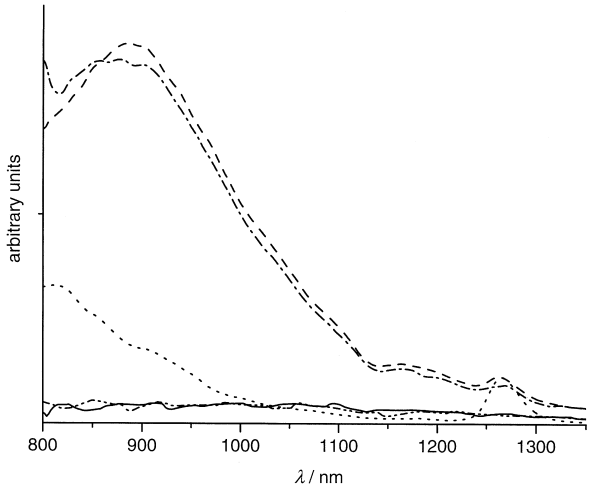

Figure 10. Corrected emission spectra in the infrared spectral region at 298 K of: **4** (····) in toluene, **1·Zn** in toluene (•–•–) and benzonitrile (——), **2·Zn** in toluene (- - - -) and benzonitrile (– ·· –), upon excitation at 488 nm (argon ion laser, $E = 0.2$ W), $A = 0.150$. For **4**, the sensitized luminescence of singlet oxygen at 1270 nm is evidenced.

The detection of the luminescence decay profiles for **1·Zn** and **2·Zn** is made difficult by their spectral position. In fact, both display a fullerene-based luminescence, strongly reduced with respect to model compounds (Figures 8 and 9), in the 700 – 850 nm spectral region, accompanied by their peculiar IR luminescence above 850 nm (Figure 10). The former bands are in a spectral region detectable either by the single photon spectrometer and the streak camera apparatus, but the signals are very weak; the latter is peaked in a region were both instrumentation have scarce or no detection. Everything considered, the most reliable equipment for detecting luminescence lifetimes is the streak camera, by which one can associate to a given decay the corresponding spectral profile, but taking into account that 860 nm is definitely the limit for signal detection. By analyzing the decays of the streak image of **2·Zn** at 700 and 860 nm, we found $\tau_1 = 1400$ ps and $\tau_2 = 730$ ps, respectively (Figure 11). For **1·Zn**, one can safely assign a lifetime of 1460 ps at 805 nm but, at 860 nm, the tail of the higher-energy lying band prevents a selective analysis.

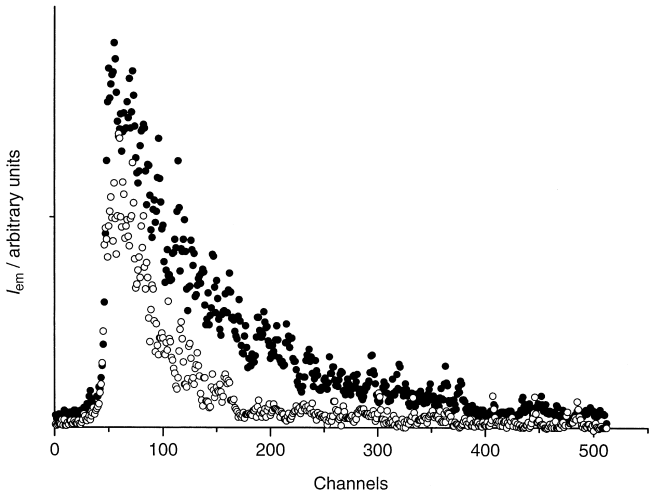

Figure 11. Luminescence decay of **2·Zn** read on the streak image at 700 (solid circles) and 860 nm (empty circles).

In rigid toluene matrix at 77 K, **1·Zn** and **2·Zn** display broad spectra with maxima centered around 730 – 740 nm (800 – 810 nm in the corrected spectra). A comparison with the spectra of the model compounds (Figure 7) clearly shows their own peculiarity: spectral features ascribable to the model porphyrin or fullerenes can hardly be found. Moreover, the 77 K luminescence decays range in a time domain not typical of the model compounds under the same conditions: **1·Zn** exhibits a relatively long, clean mono-exponential decay ($\tau = 9.5$ ns), whereas for **2·Zn**, a double exponential decay is measured ($\tau_1 = 4.2$ ns, $\tau_2 = 62.5$ ns), each component displaying the same relative amplitude. Such lifetimes were easily detected with the single photon counting apparatus. Interestingly, the luminescence spectrum of **2·Zn** (not shown) displays a shoulder around 700 nm, the only feature which could be somehow related to the fluorescence spectrum of the model compound **5**. No long-lived phosphorescence could be detected in both porphyrin – fullerene arrays.

Transient absorption spectra: The most relevant transient absorption data for all the investigated compounds are reported in Table 2. The picosecond transient absorption spectrum of **3·Zn** in toluene solution is very similar to that of ZnTPP showing a wide band in the 440 – 540 nm region on which, within our time window (3.3 ns), the singlet-to-triplet conversion can be partially evidenced; between 540 and 670 nm, the bleaching of the Q bands can also be observed. On a microsecond time scale, the fully evolved spectrum of the triplet ($\lambda_{max} = 470$ nm) can be detected; its lifetime is 560 ns and 130 μs in air-equilibrated and deoxygenated

solutions, respectively. The picosecond transient absorption spectrum of **4** is reported in Figure 12a and displays both singlet–singlet ($\lambda_{max} = 520$ and 710 nm) and triplet–triplet ($\lambda_{max} = 695$ nm) absorption features. The decay of the singlet bands matches the formation of the triplet, and isosbestic points at 560 and 710 nm are found. The lifetimes of singlet decay and triplet formation coincide and are in agreement with the singlet lifetime determined by luminescence (1.6 ns). On a longer time scale, the fully evolved triplet spectrum of **4** can be detected and shows an absorption maximum at 695 nm. The triplet lifetime is 260 ns and 30 μs in air-equilibrated and deoxygenated solutions, respectively.

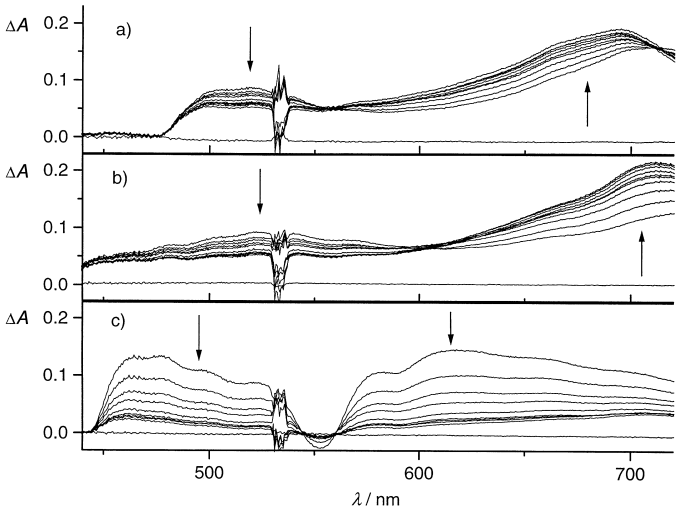

Figure 12. Picosecond transient absorption spectrum of a) **4**, b) **5**, and c) **2·Zn**; toluene solution; $\lambda_{exc} = 532$ nm; energy: 5 mJ per pulse; $A = 0.260$, 0.260, and 0.335, respectively; time intervals 330 ps.

The picosecond transient absorption spectrum of **5** is reported in Figure 12b. It shows both singlet–singlet ($\lambda_{max} =$ 535, 750, and 900 nm) and triplet–triplet ($\lambda_{max} = 710$ nm) absorption features. The singlet bands decay with $\tau = 1.6$ ns, in good agreement with the luminescence findings. The lowest triplet state decays with a lifetime of 280 ns and 23 μs in air-equilibrated and deoxygenated solution, respectively.

The shape of the transient absorption spectra of **1·Zn** and **2·Zn** in toluene solution at 298 K are very similar to each other and rather different from those of the model compounds (Figures 12c and 13a). The picosecond spectrum of **1·Zn** immediately after the laser pulse exhibits two broad bands separated by the Q band bleaching and decays with $\tau = 730$ ps at $\lambda = 580$ nm.

Another feature persisting on a longer time scale is evidenced around 690 nm whose lifetime, by means of the slow flash photolysis apparatus, is found to be 300 ns in air-equilibrated solution and 11 μs in oxygen-free solution. The picosecond transient absorption spectrum of **2·Zn** is very similar to that of **1·Zn** and decays with $\tau = 720$ ps at 600 nm. Again, a long-living component is detected with $\tau = 280$ ns and 2.6 μs in air-equilibrated and oxygen-free solution, respectively.

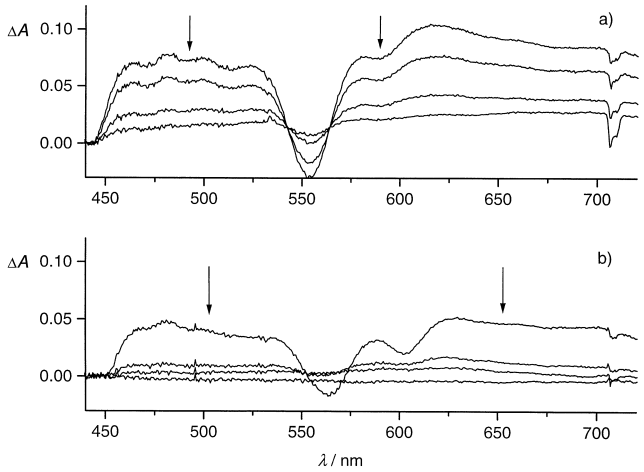

Figure 13. Picosecond transient absorption spectrum of **1·Zn** in a) toluene and b) benzonitrile solution recorded immediately after the laser pulse and at time intervals of 330, 1155, and 2800 ps. $\lambda_{exc} = 355$ nm; energy: 4 mJ per pulse; $A = 0.900$.

Singlet-oxygen sensitization: Both Zn^{II}-porphyrins[18] and fullerenes[18a, 19] are known to be strong singlet-oxygen sensitizers from the lowest triplet excited state. Experiments on sensitization of singlet oxygen ($^1\Delta_g$) were carried out by measuring the intensity of singlet-oxygen luminescence at 1270 nm in air-equilibrated toluene solution, under steady-state light irradiation ($\lambda_{exc} = 488$ nm, argon ion laser). Taking as standard plain C_{60}, which displays a singlet oxygen sensitization yield Φ_Δ equal to 1.0[18a, 20] in toluene solution, we measured values of 0.80 for **3·Zn** and **5** and 0.50 for **4**. Conjugates **1·Zn** and **2·Zn** only show a faint luminescence peak at 1270 nm, hardly distinguishable over the tail of the broad IR luminescence band (Figure 10); relative to C_{60}, its intensity is estimated to be ~ 0.10.

Discussion

Photophysics of model compounds 3·Zn, 4, and 5: The photophysical properties of **3·Zn** in the ground and excited state at 298 or 77 K (absorption and emission spectra, luminescence quantum yields, excited state lifetimes, etc.) are identical, within the experimental uncertainty, to those of ZnTPP under the same conditions.[16] This is an expected result since the malonate side chains on the *meso*-phenyl rings do not affect the delocalization of the π-system.

The *trans*-1 bis-methanofullerene **4** displays ground state absorption spectral features rather different to those of the mono-methanofullerene **5** (Figure 3) and plain C_{60};[16] consequently the color of these species in toluene solution changes from bright purple (C_{60}), to red-brownish (**5**), to deep yellow (**4**). Mono-adduct **5** is the stronger emitter of the series, with fluorescence quantum yields (Φ_{em}) more than doubled relative to **4** and C_{60}. Interestingly, also the excited state lifetimes (τ) significantly differ in the three cases, thus leading to variations of the radiative deactivation rate constants [Equation (1)] of the lowest singlet excited state, which equals

$$k_r = \frac{\Phi_{em}}{\tau} \quad (1)$$

0947-6539/00/0609-1636 $ 17.50+.50/0 *Chem. Eur. J.* **2000**, *6*, No. 9

to $1.3 \times 10^5\ s^{-1}$ (**4**), $2.9 \times 10^5\ s^{-1}$ (**5**), and $1.5 \times 10^5\ s^{-1}$ (C_{60}). Interestingly, and probably for the first time,[21] a fullerene derivative with radiative rate constant comparable (or even lower) to that of plain C_{60} is reported here. The identical fluorescence quantum yields exhibited by **4** and C_{60},[16] suggests that non-radiative rate constants are also comparable in the two cases, which is somewhat surprising on the basis of the so-called energy gap law,[22] considering that the energy difference between the involved excited singlets is over 2000 cm^{-1}. The lack of phosphorescence in **4** and **5**[16] is typical for C_{60} and lower adducts, where phosphorescence bands have been detected only below 5 K[23] or in the presence of heavy-atom containing solvents.[24]

The decrease in the singlet oxygen sensitization yield (Φ_Δ) from C_{60} (1.0), to **5** (0.80), to **4** (0.50) is in line with previous reports, that show a decrease of Φ_Δ upon increasing the number of addends on the fullerene sphere.[24a, 25]

In order to gain insight into the nature of the excited states of the fullerene derivative **4** (those of **5** and C_{60} have already been discussed[16, 17a]), we carried out a series of semi-empirical calculations. The electronic states of bis-adduct **4** were calculated starting from MM+ optimized geometries using the ZINDO/S (Zerner intermediate neglect of differential overlap/spectroscopic) program included in the Hyperchem package[26] (the CI was fixed to 14×14 MOs). The calculated spectrum, as far as the electronic transitions are concerned, is shown in the inset of Figure 3 and is in good agreement with the experimental one. In particular, the first singlet states, calculated at 773 and 695 nm, respectively, are totally centered on the fullerene part of the molecule and do not show any sizable oscillator strength (f), in agreement with the fact that the substituents decrease the high molecular symmetry of C_{60} (I_h), without destroying it completely. The long absorption tail in the 500 – 700 nm region is probably due to vibronic coupling with upper states, which is the main responsible for the fluorescence of C_{60} and its derivatives.[27] The first sizable singlets are calculated at 464 ($f = 0.014$) and 431 nm ($f = 0.007$), and this fits well with the doublet of sharp bands detected in this spectral region (Figure 3). These two bands can be interpreted as derived from the splitting and red-shifting of the first allowed band of C_{60} (404 nm); however, while the band around 430 nm is common for C_{60} mono-adducts,[28] that at 460 nm looks more specific of this symmetric bis-adduct, independent of the nature of the addends which, in this case, present much higher-lying permitted states. Also, the trend in the decrease of the singlet energy upon increasing the number of addends is well reproduced; in fact calculated values of 773 and 692[16] nm are found for **4** and **5**, respectively, to be compared with 804 and 694 nm, as obtained from the maxima of the 77 K fluorescence spectra.

Photophysics of the dyads 1·Zn and 2·Zn

Ground-state absorption, steady-state, and time-resolved luminescence: The comparison between the absorption spectra of **1·Zn** and **2·Zn** with the sum of the corresponding component units (Figures 4 and 5) is very interesting. In particular, one can note that: i) in the UV the profiles are very well matched; ii) the Soret bands are considerably depressed and red-shifted; iii) the Q bands are slightly less intense even though they get some contribution from the underlying fullerene bands; iv) solvent-dependent spectral broadening towards the low-energy side is clearly evidenced, with a tail up to 800 nm (toluene) or 850 nm (benzonitrile), totally absent in the sum spectra.

The good matching in the UV spectral portion, where the fullerene absorptions strongly prevail, suggests that the high-energy electronic transitions of the fullerene moieties are little or not affected in the porphyrin – fullerene arrays; by contrast, remarkable influence is evidenced on the porphyrin transitions. In particular, the effect on the Soret bands is substantial and unambiguously shows the influence of the nearby fullerene electron acceptor on the porphyrin electronic states. It is worth noticing that direct coordination of an electron *donor* ligand (i.e., pyridine)[16, 29] to the zinc ion of a Zn^{II} porphyrin is known to shift the Soret band to the red. In our case, where the interaction is with an electron *acceptor*, both a red-shift and a strong intensity decrease are observed. This result can be somehow expected in the case of **1·Zn**, where the fullerene moiety is forced to face the porphyrin macrocycle at close interchromophoric distance. Interestingly, however, the absorption data for **2·Zn** also suggest that in this more flexible system at least one of the two fullerenes is in very close distance of the porphyrin chromophore. Thus, the spectral data provide further support for the preferred geometry of **2·Zn** depicted in Figure 2 which had been proposed on the basis of the NMR data (see above). Indeed, an optimized three-dimensional structure (MM+) provides further support for this geometry. The minimum calculated distances between the Zn atom and the fullerene surface are fairly similar for **1·Zn** and **2·Zn** (in the conformation schematically depicted in Figure 2), amounting to 3.9 and 4.1 Å, respectively. Moreover, both structures show a very crowded area around the face of the porphyrin macrocycle which interacts with the fullerene, allowing only a limited amount of solvent molecules around it. The similar geometric relationship between porphyrin and fullerene chromophore in the two conjugates is reflected in the similar, and in a sense unexpected, behavior with respect to the spectroscopic properties and, as we will see, in the patterns of photoinduced processes.

As far as the absorption spectral tail extending toward the low-energy side is concerned, it must be pointed out that to date several cases of face-to-face Zn^{II}-porphyrin/acceptor systems have been published,[8] but invariably no low-energy absorption features were found. The same can be said about covalently linked porphyrin – fullerene systems, where the experimental absorption spectrum is typically the plain superimposition of the component units.[3a, 30] In contrast, some authors report on ground (and also excited) state interactions between fullerenes and organic electron donors such as aliphatic or aromatic amines,[31] that lead to a broadening of the fullerene absorption spectrum towards the near infrared region. On the basis of these observations, and taking into account the complementary electronic donor – acceptor properties of the involved partners, we propose that the low-energy absorption tails exhibited by

1·Zn and **2·Zn** could be an indication for *ground state* charge-transfer interactions. Such interactions are promoted by the favorable geometrical arrangement which allow the donor and the acceptor moieties to stay close to each other, and were not found by simply mixing the reference compounds in the proper ratio. In this case, the experimental spectrum was found to be identical to the sum of the spectra of the component units. This is also the case for a related face-to-face "parachute-type" dyad where the fullerene and the porphyrin fragments are well separated by the malonate linking unit.[5d]

For **1·Zn** and **2·Zn**, clear evidence was obtained for the presence of porphyrin–fullerene charge-transfer interactions in the excited state. In fact, *both* the porphyrin *and* the fullerene fluorescence are (to a different extent) quenched, while a new emission band in the infrared spectral region is recorded in toluene solution, attributable to a low-lying CT state. The quenching of the porphyrin fluorescence at 298 K (Figure 6) is complete and very fast. Indeed, no traces of residual short-lived fluorescence were found within our time resolution (20 ps), enabling us to only estimate a lower limiting value of $5 \times 10^{10}\ s^{-1}$ for the quenching rate constant from Equation (2):

$$k = 1/\tau - 1/\tau_0 \sim 1/\tau \qquad (2)$$

where τ and τ_0 are the lifetimes of the quenched (limiting value of 35 ps) and unquenched (reference compound **3·Zn**) moiety.

On the other hand, the fluorescence of the fullerene moieties is not completely quenched in intensity and the corresponding lifetime is only very little affected. At first glance, Figures 8 and 9 seem to indicate that the residual fullerene-centered fluorescence in **1·Zn** is more intense than in **2·Zn** but this is only an artifact due to the fact that in **1·Zn** this band is considerably red-shifted relative to the emission of **2·Zn**. As a consequence, it receives a larger contribution from the IR-centered emission band (Figure 10) which, towards the high-energy side, is likely to extend up to the 700–800 nm spectral region. Of course this effect is reciprocal, as one can see by inspecting the IR spectrum of **1·Zn** between 800 and 850 nm (Figure 10), and compare it with that of **2·Zn**. Such spectral overlap is also likely to be responsible for the lower resolution observed for the fluorescence spectra of **1·Zn** and **2·Zn** relative to their model compounds (Figures 8 and 9). Owing to this spectral superimposition and the impossibility of selective excitation, it is difficult to evaluate the actual amount of residual fullerene fluorescence. Nevertheless, in the more favorable case of **2·Zn** (less pronounced spectral overlap), one can roughly estimate a residual amount of fullerene singlet excited state around 15%. In any case, the excitation spectra of **1·Zn** and **2·Zn** taken at 805 nm show the typical spectral features of the porphyrin moiety, including the diagnostic Soret bands in their peculiar spectral position, thus showing that the porphyrin fluorescence is quenched by energy-transfer to the lower-lying CT or fullerene singlet states. The same mechanism can be expected to be active in a rigid matrix at 77 K where dramatic fluorescence quenching is also detected; moreover the lack of porphyrin phosphorescence clearly demonstrates that the intersystem crossing deactivation pathway to the lowest triplet state is suppressed.

In order to get further insight into the contemporary presence of a residual fullerene fluorescence and a new CT luminescence band, one can try to take advantage of their different spectral position and, via a streak camera device, analyze the corresponding decay profiles. As briefly discussed in the result section, this can be safely done only for **2·Zn** and not for **1·Zn** since in the former the spectral separation between the fullerene fluorescence and the CT band is larger. For **2·Zn**, we found two distinct decays at 700 and 860 nm with $\tau = 1400$ and 730 ps attributable to the residual fullerene singlet and CT states, respectively (Figure 11), the longer lifetime being slightly shorter than that of the reference compound **5** (1.7 ns). Also for **1·Zn**, a long-lived decay is observed at 805 nm (1460 ps), slightly shortened in comparison with the reference compound **4**. More reliable data for the CT state in **1·Zn** can be obtained from the transient absorption spectroscopy, see below.

As it happens at room temperature, the luminescence behavior of **1·Zn** and **2·Zn** at 77 K is completely different with respect to that of the model compounds (Table 2 and Figure 7). Very broad, blue-shifted (relative to 298 K) bands are found, associated with relatively long-lived decays; the spectral shift to higher energy ($1500\ cm^{-1}$) is another clue to the charge-transfer character of the lowest excited state. For **2·Zn**, the luminescence decay is doubly exponential ($\tau_1 =$ 4.2 ns, $\tau_2 = 62.5$ ns), each lifetime displaying the same relative amplitude. This suggests that different degrees of porphyrin–fullerene interactions are present in the frozen matrix, and indicates that the behavior of **1·Zn** and **2·Zn** is no longer identical under these conditions. Very important, the spike observed for the luminescence spectrum of **2·Zn** around 700 nm demonstrates that some residual fullerene-centered singlet is also present at 77 K.

Transient absorption spectroscopy: A detailed analysis of the picosecond transient absorption spectra at 298 K gives further support to the proposed charge-transfer nature of the lowest excited states in **1·Zn** and **2·Zn**. The spectra of the two molecules, taken immediately after the laser pulse (35 ps duration), are very similar to each other and hardly remind those of the model compounds (Figures 12 and 13a). The lack of contribution from the porphyrin moiety, instantaneously quenched, is expected on the basis of the luminescence findings but, clearly, also the fullerene moiety, albeit not completely quenched, does not seem to contribute significantly to the immediate spectral profile. For instance, one can compare the spectra of **5** and **2·Zn** (Figure 12b,c) at 605 nm where the former shows an isosbestic point and the latter a maximum. Such marked differences, by the way, cannot be justified on the basis of the difference between the corresponding ground state absorption spectra (see Figures 3–5).

Importantly, for **1·Zn** and **2·Zn**, the large bands in the range between 600 and 700 nm can be attributed to the porphyrin radical cation, in agreement with several previous reports.[32] Furthermore, the transient absorption spectra of **1·Zn** and **2·Zn** decay with $\tau = 730$ and 720 ps, respectively, at

0947-6539/00/0609-1638 $ 17.50+.50/0 *Chem. Eur. J.* **2000**, *6*, No. 9

605 nm. For **2·Zn**, an identical lifetime (within the experimental uncertainty) is found for the IR luminescence, indicating that the same species is unambiguously monitored by the two techniques, namely the low-lying charge-transfer state.

The picosecond transient absorption spectra of **1·Zn** and **2·Zn** also exhibit, around 700 nm, some features that persist in the explored time window (about 3000 ps), only decaying on a longer (microsecond) time scale. They can be attributed, in analogy with the spectra of the reference compounds, to a residual amount of fullerene triplet. A quantitative estimation of such a residue can be attempted, by comparison with the proper model compounds, either by monitoring the nanosecond transient absorption at $\lambda_{abs} = 700$ nm or by evaluating the amount of sensitized singlet-oxygen luminescence (Figure 10) at 1270 nm. For several reasons, including signal weakness, both methods are subject to large experimental uncertainties. However, such residue can be roughly estimated to be of the order of 15 %.

Proposed model and photoinduced processes: Our spectroscopic investigations clearly give evidence for some residual amount of fullerene localized excited states. A comparison with the corresponding proper model compounds shows that the relative amount of residual singlet or triplet is identical (about 15 %), as detected via luminescence and/or transient absorption spectroscopy (see above). Moreover, very importantly, only the intensity of the detected signal is decreased whereas the lifetimes, at least in air-equilibrated solution, are negligibly or not affected. All these data suggest that the observed residual triplet is generated by intersystem crossing from the lowest excited singlet (which is known to occur with unitary efficiency in C_{60}[20, 33]) in the minority fullerene-centered excited states. These experimental findings indicate that in **1·Zn** and **2·Zn**, a (minor) fraction of molecules is not involved in excited state charge-transfer interactions in toluene as the solvent. This could imply that an equilibrium between "tight" and "loose" porphyrin/fullerene pairs is established in the ground and/or excited state, and only in the tight pairs a significant CT interaction can be set up. "Tight" and "loose" porphyrin/fullerene pairs differ in the distance between donor and acceptor and also in their solvation environment. Indeed one could object that the two observed photophysical behaviors could not be due to an equilibrium between conformationally different molecules, but simply to a thermal equilibrium between the local (fullerene singlet) and the CT excited states in conformationally identical molecules. This hypothesis can be ruled out because it cannot explain the observed identical relative yields of fullerene singlet and triplet. Furthermore, the presence of a residual amount of fullerene fluorescence at 77 K hardly fits with thermally activated equilibria. Finally, it is worthwhile to point out that in **2·Zn**, the fullerene unit not sitting in tight face-to-face contact with the porphyrin fragment (Figure 2) is not expected to give a substantial contribution to the observed spectroscopic patterns. In fact such a moiety, upon direct photoexcitation to the lowest singlet excited state, is expected to be quenched by the lower-lying CT level localized on the nearby contact pair.

Quite interestingly, the triplet lifetimes of the fullerene-centered excited states of **1·Zn** and **2·Zn** are substantially reduced, but in oxygen-free solution only. This is particularly evident for **2·Zn**, where the triplet lifetime is 2.6 μs, to be compared with 23 μs for reference compound **5**. This suggests that a dynamic quenching of the (residual) fullerene triplet in **2·Zn** occurs, with a rate constant of $3.8 \times 10^5\ s^{-1}$ [see Eq. (2)]. This could be a consequence of the above-proposed dynamic equilibrium that, on such a long (microsecond) time scale, would allow the deactivation of the formerly localized fullerene triplet state to the lower-lying charge-transfer level, then made available. This triplet quenching is slower for **1·Zn**, since thermodynamically disfavored or even thermally activated, given the position of the triplet excited state of **4** (1.30 eV) and **5** (1.57 eV) relative to the corresponding CT excited state level, see Figures 14 and 15.

The construction of an energy level diagram for **1·Zn** allows to summarize the porphyrin – fullerene intercomponent processes occurring upon light irradiation (Figure 14). In this Figure, the lowest lying porphyrin and fullerene singlet and triplet excited states are reported, whose energy was obtained from the highest lying 77 K emission band feature or, when not available as in the case of the fullerene triplet, from theoretical calculations. The position of the charge-transfer state is obtained from electrochemical data[34] in CH_2Cl_2 because electrochemistry could not be carried out in toluene solution, whereas photophysical investigations in CH_2Cl_2 are difficult to perform due to the photochemical instability of Zn^{II}-porphyrin derivatives in chlorinated solvents. In Figure 14, the processes concerning tight pairs (where a CT interaction is established) and loose pairs (only locally excited states involved) are reported with dashed and full lines; the rates of internal conversion and intercomponent processes are obtained from the reciprocal of the excited state lifetimes (air-equilibrated solutions) as in Equation (2).

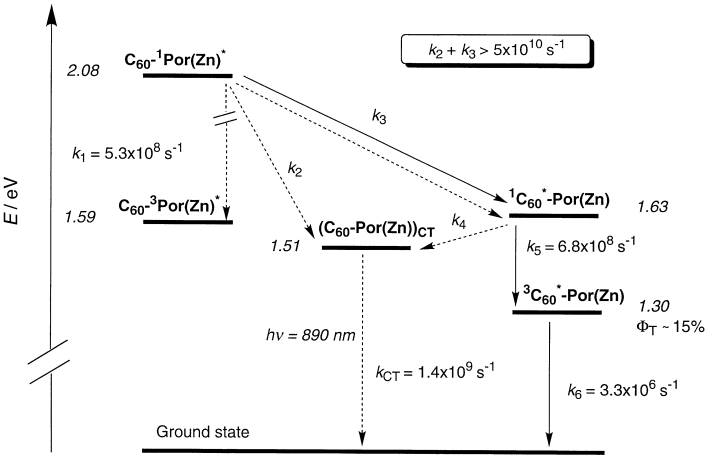

Figure 14. Energy-level diagram describing the excited state deactivation pathways and the intercomponent processes in **1·Zn** in air-equilibrated toluene solution. On the left-hand side are located the lowest electronic singlet and triplet excited states centered on the porphyrin moiety, on the right hand side the lowest electronic singlet and triplet excited states centered on the fullerene fragment. $(C_{60}-Por(Zn))_{CT}$ in **1·Zn** represents the lowest-lying charge-transfer excited state, luminescent in toluene solution. In benzonitrile such CT state is located at 1.38 eV and does not luminesce. Dashed and full arrows, respectively, represent processes occurring in molecules where CT interactions are established or not.

For tight pairs, the internal deactivation of $C_{60}-{}^1Por(Zn)^*$ in **1·Zn** ($k_1 = 5.3 \times 10^8\ s^{-1}$) cannot compete with the intercomponent energy transfer to the CT and also fullerene centered singlet ${}^1C_{60}^*-Por(Zn)$ in **1·Zn** ($k_2+k_3 > 5 \times 10^{10}\ s^{-1}$). Of course, for loose pairs only the latter process is made possible ($k_3 > 5 \times 10^{10}\ s^{-1}$). The value of the energy-transfer rate k_4 could not be determined since the weak and short-lived quenched fullerene fluorescence is masked by the unquenched long-lived component, and also in view of the unfavorable spectral position (vide supra). The rate of charge-transfer decay ($k_{CT} = 1.4 \times 10^9\ s^{-1}$) is obtained from the picosecond transient absorption data. Finally, the internal conversion rates for fullerene locally excited state (k_5 and k_6) are substantially unaffected relative to the reference compounds. The analogous Scheme for **2·Zn** (Figure 15) can be described with similar arguments.

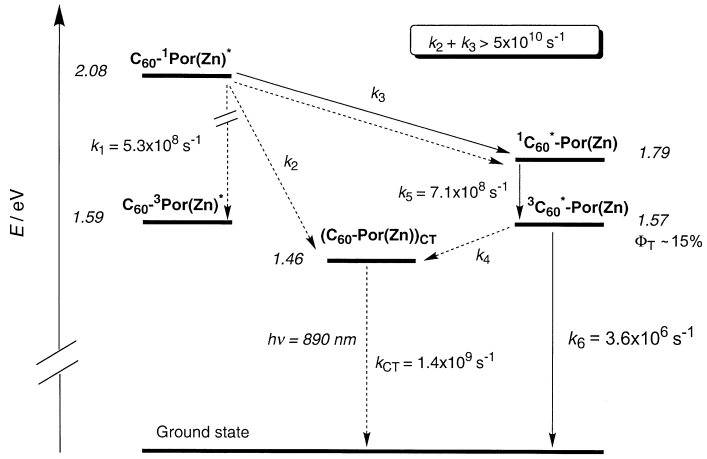

Figure 15. Energy-level diagram describing the excited state deactivation pathways and the intercomponent processes in **2·Zn** in air-equilibrated toluene solution. On the left-hand side are located the lowest electronic singlet and triplet excited states centered on the porphyrin moiety, on the right hand side the lowest electronic singlet and triplet excited states centered on the fullerene fragments. $(C_{60}-Por(Zn))_{CT}$ in **2·Zn** represents the lowest-lying charge-transfer excited state, luminescent in toluene solution. In benzonitrile such CT state is located at 1.33 eV and does not luminesce. Dashed and full arrows represent processes occurring in molecules where CT interactions are established or not.

Current electron-transfer theory[35] allows the estimation of the extent of donor–acceptor electronic coupling through the H_{DA} parameter which is included in the quantum mechanical expression of the electron-transfer rate k_{el} in Equation (3):

$$k_{el} = \frac{2\pi}{\hbar} H_{DA}^2\ \mathrm{FCWD} \qquad (3)$$

where H_{DA} is the electronic matrix element that mixes the donor and the acceptor states and FCWD is the Franck–Condon weighted density of states.

Under proper approximations, it is possible to calculate H_{DA}[35, 36] (in cm^{-1}) either from absorption in Equation (4):

$$H_{DA} = \frac{2.06 \times 10^{-2} \sqrt{\varepsilon_{max}\, \nu_{max}\, \Delta\nu_{1/2}}}{R_c} \qquad (4)$$

or emission parameters in Equation (5)

$$H_{DA} = \sqrt{\frac{1.4 \times 10^5\, k_F}{n^3\, R_c^2\, \nu_{CT}}} \qquad (5)$$

where ε_{max} and ν_{max} represent the molar extinction coefficient (in $M^{-1}\,cm^{-1}$) and frequency (in cm^{-1}) of the CT absorption, $\Delta\nu_{1/2}$ (in cm^{-1}) is the full width at half height, R_c (in Å) the center to center distance, k_F (in s^{-1}) is the radiative deactivation rate constant of the CT excited state, n is the solvent refractive index, and ν_{CT} (in cm^{-1}) the frequency of the CT emission maximum.

In our case, Equation (5) cannot be applied since the k_F value is not available, owing to the lack of the emission quantum yield value for the CT band (Table 2); therefore a (rough) H_{DA} estimation can be attempted only from absorption data. In the case of **1·Zn**, from the spectrum of Figure 4, one can estimate the following parameters: $\varepsilon_{max} = 50\ L\,mol^{-1}\,cm^{-1}$, $\nu_{max} = 15\,000\ cm^{-1}$, $\Delta\nu_{1/2} = 4000\ cm^{-1}$. Putting these data in Equation (4) and taking $R_c = 4$ Å (minimum distance from the porphyrin to the fullerene surface, according to molecular modeling), an H_{DA} value of $280\ cm^{-1}$ is obtained, indicating a donor–acceptor interaction of intermediate strength.[37]

Spectroscopic investigations in benzonitrile solution: In order to test our interpretation of the photophysical behavior in toluene solution (dielectric constant 2.4), we performed a series of spectroscopic investigations in the more polar benzonitrile solvent (dielectric constant 25.2).

The reference compounds **3·Zn**, **4**, and **5** in benzonitrile solution exhibit spectroscopic properties such as steady-state and transient absorption spectra, luminescence properties, and excited-state lifetimes very similar, if not identical, to those in toluene solution. By contrast, the photophysical behavior of **1·Zn** and **2·Zn** is very different from that observed in toluene solution. The most remarkable differences are the following:

i) a broader and more intense tail of the steady-state absorption spectra toward the low-energy side (Figures 4 and 5);
ii) no residual fullerene fluorescence at 298 K;
iii) no luminescence bands at 77 K;
iv) no luminescence in the near infrared (Figure 10);
v) no singlet-oxygen sensitization (Figure 10);
vi) no long-lived transient absorption around 700 nm on the nano- and microsecond time scale;
vii) a shorter decay of the picosecond transient absorption spectra, that is 100 ps and 350 ps for **1·Zn** (Figure 12) and **2·Zn**, respectively; the spectral shape is similar to that in toluene.

On the basis of these observations one can obtain a number a valuable indications:

a) The broadening of the steady-state absorption spectra could suggest that ground state charge-transfer interactions are present and even lower-lying than in toluene, as expected in a more polar medium;
b) the lack of fullerene fluorescence and of a long-lived transient absorption signal demonstrate that the formation of localized excited states is not allowed; in other words, in a polar solvent only tight CT pairs are formed;
c) picosecond transient absorption spectra show that the lowest excited state of **1·Zn** and **2·Zn** possesses a CT character, since the typical features of the porphyrin

0947-6539/00/0609-1640 $ 17.50+.50/0 *Chem. Eur. J.* **2000**, *6*, No. 9

radical cation are observed, as in toluene solution (vide supra).

The lack of any luminescence in the near IR spectral region and the short excited state lifetime (shorter than in toluene) are a consequence of the low energy of the charge-transfer state in a polar environment, that tends to favor fast, radiationless deactivation owing to the already mentioned energy-gap law.[22] Accordingly the charge transfer state energy, as obtained from electrochemical data, is positioned at 1.38 and 1.33 eV for **1·Zn** and **2·Zn**, respectively; such values, corresponding to $\lambda > 900$ nm, can be safely located in a non-emissive domain.[38]

Again, on the basis of Equation (4), one can estimate H_{DA} for **1·Zn**. Owing to a four-fold increase in the ε_{max} ($\sim 200\ M^{-1}\ cm^{-1}$), H_{DA} turns out to be 570 cm^{-1}, that is twice the value calculated in toluene, thus showing a stronger electronic coupling in the polar medium.

Conclusion

In an attempt to strengthen porphyrin – fullerene electronic interactions by forcing them to stay close to each other, we synthesized the cyclophane-type molecular dyad **1·Zn**, with a *trans*-1 fullerene addition pattern, in which both chromophores are rigidly held at van der Waals distance in a tangential orientation. As a side product, compound **2·Zn** with two C_{60} moieties appended to the porphyrin ring by single linkers, was obtained. NMR investigations showed that this compound strongly prefers conformations with one of the carbon spheres nesting on the porphyrin surface, thereby taking a similar orientation to that seen in doubly bridged **1·Zn**. This explains the remarkable, and initially quite unexpected, similarity in the electrochemical and photophysical properties. Electrochemical measurements of these dyads as well as of the corresponding free-base porphyrins **1·2H** and **2·2H** showed only small redox potential shifts induced by the C_{60} sphere on the adjacent porphyrin and vice versa. On the other hand, steady-state electronic absorption spectra of **1·Zn** and **2·Zn** exhibit large changes in comparison to the model porphyrin **3·Zn** and the model fullerene derivatives **4** and **5**, respectively. The Soret band of the porphyrin in the dyads is substantially red-shifted, and new broad tails are observed in the near infrared region. We take this as evidence for donor – acceptor interactions in **1·Zn** and **2·Zn** in the ground state. Strong CT interactions are clearly evidenced in the excited state using time-resolved absorption and luminescence spectroscopy. The electronic donor – acceptor interactions between the porphyrin and the fullerene units in the two dyads are strongly solvent dependent. In toluene, a minor fraction of **1·Zn** or **2·Zn** (around 15 %) is not involved in donor – acceptor interactions. Interestingly, and to our knowledge for the first time, the porphyrin – fullerene charge-transfer interaction gives rise to a low-lying luminescent state, its emission band being located in the near infrared region (λ_{max} around 890 and 800 nm at 298 and 77 K, respectively) with $\tau = 730$ ps in toluene. In benzonitrile, such a CT state is still present but it is shorter lived and not luminescent, since the polar environment lowers its energy so that non-radiative deactivation pathways prevail. Importantly, there is no substantial difference between the photophysical behavior of **1·Zn** and **2·Zn**. This demonstrates that similar fullerene – porphyrin interactions[15] exist in the two cases and provides strong support for a preference of **2·Zn** for conformations with one fullerene moiety nesting on the porphyrin (Figure 2).

In conclusion, this work suggests two new approaches for the construction of photoactive porphyrin – fullerene arrays. Charge transfer in the excited state and possibly also in the ground state can be reached by fixing donor and acceptor at van der Waals distance in rigid cyclophane-type structures such as **1·Zn**. Alternatively, strong fullerene – porphyrin interactions may enforce a strong preference of singly bridged systems such as **2·Zn** for conformations, in which donor and acceptor adopt a close spatial relationship similar to that established in the cyclophane-type dyad. Remarkably, both ways of controlling spatial interchromophoric orientation and alignment can lead to nearly identical photophysical properties. Future applications of these design criteria to the construction of photochemical molecular devices are now being tested in view of the interesting possibilities for practical applications.[3]

Experimental Section

General: Reagents and solvents were purchased as reagent grade and used without further purification. C_{60} (99.5 %) was purchased from Southern Chemical Group, LLC, Tucker, GA 30085-0527, USA. CH_2Cl_2 was dried over CaH_2. Compounds **4**,[10] **5**,[11] **6**,[13] and **8**[14d] were synthesized according to literature procedures. All reaction were performed in standard glassware under Ar. Evaporation and concentration in vacuo were performed at water-aspirator pressure, and compounds were dried at 10^{-2} Torr. Flash chromatography (FC): SiO_2-H, 5 – 40 μm, Fluka, with elution at 0.2 – 0.4 bar; SiO_2 60, 0.063 – 0.2 μm, Fluka, with elution at a maximum pressure of 0.1 bar. TLC: Alugram SIL G/UV_{234}, Macherey – Nagel, visualization by UV light at 254 nm. M.p.: Büchi B-540 apparatus, uncorrected. UV/Vis spectra: Varian Cary-5 spectrophotometer. Fluorescence: Fluorolog Spex 1680 spectrometer. IR Spectra: Perkin – Elmer 1600 FTIR. NMR spectra: Bruker AM 500 and Varian Gemini 300 or 200, with solvent peaks as reference. MS (FAB): VG ZAB 2SEQ instrument; 3-nitrobenzyl alcohol as matrix. MS (MALDI-TOF): Bruker-Reflex TM-MALDI-TOF instrument, 2-(4-hydroxyphenylazo)benzoic acid (HABA) as matrix.

3-(Ethoxycarbonylacetoxymethyl)-benzaldehyde (7): Ethyl malonyl chloride (2.05 mL, 16.1 mmol) was added at 0 °C to a solution of **6** (2 g, 14.7 mmol) and Et_3N (2.25 mL, 16.1 mmol) in dry CH_2Cl_2 (100 mL), and the solution was subsequently stirred for 1 h at 20 °C. After addition of a saturated aqueous solution of $NaHCO_3$, the mixture was extracted with CH_2Cl_2 (3 ×). The organic layers were washed with H_2O, dried ($MgSO_4$), and evaporated in vacuo. FC (SiO_2; CH_2Cl_2/EtOAc 98.5:1.5 or PhMe/EtOAc 8:2) gave **7** as a colorless oil (3.2 g, 87 %). This compound is unstable even at −20 °C and should not be heated. IR (KBr): 2984, 2733, 1732, 1609, 1583, 1448, 1371, 1300, 1333, 1279, 1147, 1032, 894, 850, 794, 750, 694, 650 cm^{-1}; ^1H NMR (500 MHz, $CDCl_3$, 298 K): $\delta = 10.06$ (s, 1H), 7.91 – 7.53 (m, 4H), 5.29 (s, 2H), 4.23 (q, $J = 7.1$ Hz, 2H), 3.47 (s, 2H), 1.28 (t, $J = 7.1$ Hz, 3H); ^{13}C NMR (75.45 MHz, $CDCl_3$, 298 K): $\delta = 192.23$, 166.65, 166.60, 136.97, 136.85, 134.23, 129.99, 129.62, 129.33, 66.37, 61.82, 41.61, 14.06; MS (EI) m/z (%): 250 (2) $[M]^+$, 249 (10) $[M-H]^+$, 248 (50) $[M-2H]^+$, 135 (100), 119 (24); MS (HR-FAB): m/z: 250.0844 $[M]^+$; calcd for $C_{13}H_{14}O_5$: 250.0841.

10,20-Diphenylporphyrin-5,15-diylbis(1,3-phenylene)dimethanol (9): To an oxygen-free solution of pyrrole (537 mg, 8 mmol), **6** (545 mg, 4 mmol), and benzaldehyde (424 mg, 4 mmol) in CH_2Cl_2 (1 L), TFA (0.62 mL, 8 mmol) was added dropwise. After stirring at 20 °C for 24 h, DDQ (1.8 g, 8 mmol) was added and stirring was continued for 1 h. The solution was

neutralized by addition of Et_3N until pH 8, then passed through a short plug of SiO_2, washing first with $CHCl_3$ to remove the tetra(*meso*-phenyl)-porphyrin and porphyrin with three *meso*-phenyl and one *meso*-(3-hydroxymethyl)phenyl rings and then with CH_2Cl_2/EtOAc 95:5 to recover **9** together with its regioisomer. The two compounds were separated by FC (SiO_2; CH_2Cl_2/EtOAc 95:5) to yield **9** (43 mg, 3%). M.p.: 390 °C (dec., CH_2Cl_2/hexane); IR (KBr): 3400, 1594, 1561, 1472, 1350, 1228, 1194, 1150, 1033, 1000, 972, 800, 727, 700, 661, 639 cm^{-1}; ^1H NMR (500 MHz, $(CDCl_2)_2$, 298 K): $\delta = 8.80$ (d, $J = 4.7$ Hz; 4H), 8.79 (d, $J = 4.7$ Hz; 4H), 8.16–8.09 (m, 8H), 7.74–7.68 (m, 10H), 4.92 (s, 4H), −2.92 (br s, 2H); ^{13}C NMR (125.8 MHz, $(CDCl_2)_2$, 380 K): $\delta = 147.12$, 147.05, 142.73, 142.45, 139.78, 134.78, 134.07, 133.28, 131.33, 131.21, 127.97, 127.10, 126.89, 126.45, 120.50, 120.18, 65.60; MS (FAB): *m/z* (%): 675.4 (100) $[MH]^+$; MS (HR-FAB): *m/z*: 675.2761 $[M]^+$; calcd for $C_{46}H_{35}N_4O_2$: 675.2760.

1,1′-[10,20-Diphenylprophyrin-5,15-diylbis(1,3-phenylene)dimethylene] 3,3′-diethyl bis(malonate) (3·2H):

Method A: A solution of **7** (0.51 g, 2.0 mmol) and **8** (0.45 g, 2.0 mmol) in CH_2Cl_2 (500 mL) was purged with Ar, and TFA (0.16 mL, 2.0 mmol) was added. The mixture was stirred at 20 °C for 24 h, then chloranil (1.00 g, 4.0 mmol) was added. The solution was stirred for 1 h, then extracted with a saturated aqueous solution of $NaHCO_3$. The organic layer was washed with H_2O, dried (Na_2SO_4), and evaporated in vacuo. FC (SiO_2-H; CH_2Cl_2/EtOAc 98:2) yielded four dark purple fractions corresponding to the products containing four *meso*-phenyl, three *meso*-phenyl, two *meso*-phenyl (two isomers) and one *meso*-phenyl ring. The two regioisomers were separated by FC (three consecutive chromatographies; SiO_2-H; CH_2Cl_2/EtOAc 98:2) to provide **3·2H** (60 mg, 5%).

Method B: To **9** (81 mg, 0.12 mmol) and ethyl malonyl chloride (46 μL, 0.36 mmol) in dry CH_2Cl_2 (100 mL), Et_3N (37 μL, 0.26 mmol) was added dropwise at 0 °C and the solution was stirred for 1 h at 20 °C. The mixture was made basic with Et_3N and was extracted with a saturated aqueous solution of $NaHCO_3$, 1% aqueous TFA, and H_2O. The organic layer was dried ($MgSO_4$) and evaporated in vacuo. FC (SiO_2, CH_2Cl_2) afforded **3·2H** (86 mg, 80%). M.p.: 58 °C (CH_2Cl_2/hexane); UV/Vis (CH_2Cl_2): $\lambda_{max}(\varepsilon) =$ 646 (4000), 590 (5600), 550 (7900), 515 (19200), 485 (3000), 418 (443200), 401 nm (sh 83200 $mol^{-1}dm^3cm^{-1}$); fluorescence (CH_2Cl_2, $\lambda_{exc} = 418$ nm): $\lambda_{max\,em} = 649$, 714 nm; IR (KBr): 3444, 2956, 2922, 2844, 1744, 1572, 1522, 1456, 1438, 1422, 1378, 1255, 1227, 1206, 1172, 1094, 1022, 867, 800, 750, 727, 700, 661, 616, 578, 550, 522, 461 cm^{-1}; ^1H NMR (200 MHz, $CDCl_3$, 298 K): $\delta = 8.86$ (d, $J = 4.7$ Hz, 4H), 8.83 (d, $J = 4.7$ Hz, 4H), 8.25–8.20 (m, 8H), 7.79–7.75 (m, 10H), 5.50 (s, 4H), 4.12 (q, $J = 7.0$ Hz, 4H), 3.49 (s, 4H), 1.13 (t, $J = 7.0$ Hz, 6H), −2.79 (s, 2H); ^{13}C NMR (125.8 MHz, $(CDCl_2)_2$, 376 K): $\delta = 166.54$, 166.33, 147.13, 146.99, 142.81, 142.41, 134.75 (2×), 134.48, 134.17, 131.46, 131.19, 128.00, 127.50, 127.15, 126.91, 120.58, 119.79, 67.36, 61.65, 41.93, 14.18; MS (FAB): *m/z* (%): 903.2 (100) $[MH]^+$; MS (HR-FAB): *m/z*: 902.3314 $[M]^+$; calcd for $C_{56}H_{46}N_4O_8$: 902.3315.

***out,out*-61,62-Diethyl 61,62-[10,20-diphenylporphyrin-5,15-diylbis(1,3-phenylene)dimethylene] 1,2:55,60-bismethano[60]fullerene-61,61,62,62-tetracarboxylate (1·2H)**: DBU (19 μL, 0.126 mmol) was added to C_{60} (15 mg, 0.021 mmol), I_2 (12 mg, 0.046 mmol), and **3·2H** (19 mg, 0.021 mmol) in PhMe (40 mL), and the mixture was stirred for 1 h. Filtration through a small plug of SiO_2 followed by FC (SiO_2-H; PhMe/hexane 85:15) yielded three major fractions. The first one afforded pure **2·2H** (< 0.5 mg), the second the less symmetrical bis-malonate-appended regioisomer (8%, impure), and the third one pure **1·2H** (5 mg, 17%). M.p.: > 400 °C (CH_2Cl_2/hexane); UV/Vis (CH_2Cl_2): λ_{max} (ε) = 650 (2700), 595 (4300), 553 (6200), 518 (12500), 426 (198300), 410 (sh 54500), 325 (47000), 261 nm (98900 $mol^{-1}dm^3cm^{-1}$); fluorescence (CH_2Cl_2, $\lambda_{exc} = 426$ nm): $\lambda_{max} = 595$, 650, 713 nm; IR (KBr): 3432, 2956, 2911, 2856, 1749, 1467, 1439, 1367, 1344, 1243, 1206, 1167, 1090, 1072, 1016, 972, 922, 867, 799, 728, 700, 667, 633, 578, 550, 522 cm^{-1}; ^1H NMR (500 MHz, $CDCl_3$, 298 K): $\delta = 8.69$ (s, 8H), 8.64 (d, $J = 7$ Hz, 2H), 8.1–7.47 (m, 16H), 5.98 (s, 4H), 4.55 (q, $J = 7.1$ Hz, 4H), 1.50 (t, $J = 7.1$ Hz, 6H), −2.89 (s, 2H); ^{13}C NMR (125.8 MHz, $CDCl_3$, 298 K): $\delta = 163.80$, 163.74, 144.77, 144.37, 144.25, 142.99, 142.81, 142.74, 142.39, 142.29, 141.98, 141.87, 141.79, 141.43, 141.13, 140.12, 139.99, 139.66, 138.85, 135.75, 134.32 (2×), 134.26, 133.84, 132.19, 129.03, 128.22, 127.65, 126.88, 126.71, 126.54, 125.69, 120.35, 119.13, 69.33, 67.84, 63.54, 45.65, 14.30; MS (FAB): *m/z* (%): 1619.6 (100) $[MH]^+$; MS (HR-FAB): 1618.3006 $[M]^+$; calcd for $C_{116}H_{42}N_4O_8$: 1618.3002.

61,61′-Diethyl 61,61′-[10,20-diphenylporphyrin-5,15-diylbis(1,3-phenylene)dimethyl] bis(1,2-methano[60]fullerene-61,61-dicarboxylate (2·2H): DBU (22 μL, 0.144 mmol) was added to C_{60} (80 mg, 0.120 mmol), I_2 (14 mg, 0.053 mmol), and **3·2H** (22 mg, 0.024 mmol) in PhMe (50 mL) and the mixture was stirred for 1 h at 0 °C. Filtration trough a small plug of SiO_2 followed by FC (SiO_2-H; PhMe/hexane 85:15) gave **2·2H** (25 mg, 44%). M.p.: > 400 °C (CH_2Cl_2/hexane); UV/Vis (CH_2Cl_2): λ_{max} (ε) = 648 (2600), 593 (4400), 551 (6700), 517 (12600), 425 (175100), 406 (sh, 50800), 327 (66200), 259 nm (184900 $mol^{-1}dm^3cm^{-1}$); fluorescence (CH_2Cl_2, $\lambda_{exc} = 425$ nm): $\lambda_{max\,em} = 650$, 713 nm; IR (KBr): 3422, 2956, 2922, 2856, 1748, 1628, 1600, 1468, 1457, 1439, 1428, 1367, 1350, 1267, 1232, 1200, 1183, 1106, 1094, 1056, 1017, 972, 800, 728, 700, 578, 550, 526, 461, 417 cm^{-1}; ^1H NMR (500 MHz, $(CDCl_2)_2$, 298 K): $\delta = 8.74–8.68$ (m, 8H), 8.35–7.62 (m, 18H), 5.80 (s, 2H), 5.79 (s, 2H), 4.44–4.37 (m, 4H), 1.31 (t, $J = 7.1$ Hz, 3H), 1.27 (t, $J = 7.1$ Hz, 3H), −2.97 (s, 2H); ^{13}C NMR (125.8 MHz, $(CDCl_2)_2$, 298 K): $\delta = 163.80$, 163.79, 163.70, 163.67, 145.16, 145.11, 145.09, 145.01, 144.94, 144.93, 144.85, 144.82, 144.76, 144.73, 144.67, 144.55, 144.54, 144.52, 144.50, 144.37, 144.34, 144.30, 144.19, 143.79, 143.75, 143.64, 143.57, 143.41, 143.01, 142.99, 142.94, 142.84, 142.80, 142.71, 142.58, 142.53, 142.48, 142.38, 142.37, 142.13, 142.12, 142.11, 142.05, 141.96, 141.89, 141.74, 141.67, 141.55, 141.01, 140.83, 140.66, 140.59, 140.35, 140.23, 139.35 (2×), 138.25, 138.07, 135.12, 134.77 (2×), 134.53, 134.47, 133.62, 133.57, 128.08, 127.89, 127.54, 127.10, 120.71, 119.64, 119.62, 71.46, 71.39, 69.00, 68.99, 63.97 (2×), 54.08, 52.24, 14.61, 14.56; MS (FAB): *m/z* (%): 2341.1 (100) $[MH]^+$; MS (MALDI-TOF): *m/z*: 2340.1 $[M]^+$; calcd for $^{13}C_2{}^{12}C_{174}H_{42}N_4O_8$: 2340.3.

Metallation of the porphyrin derivatives: Zinc acetate (10 equivalent) was added to the porphyrin derivative (10 mM) in MeOH/$CHCl_3$ 1:1, and the solution was stirred for 1 h at 20 °C. The organic layer obtained after extraction with H_2O was dried ($MgSO_4$) and evaporated in vacuo. Filtration of the dark-purple residue through a short SiO_2 column (CH_2Cl_2) provided the corresponding Zn^{II} porphyrin derivative in quantitative yield.

1,1′-[10,20-Diphenylporphyrin-5,15-diylbis(1,3-phenylene)dimethylene] 3,3′-diethyl bis(malonate) (2-) *N*^{21}, *N*^{22}, *N*^{23}, *N*^{24} *zinc* (3·Zn): M.p.: 74–76 °C (CH_2Cl_2/hexane); UV/Vis (CH_2Cl_2): $\lambda_{max}(\varepsilon) = 585$ (2700), 548 (17500), 512 (2300), 487 (sh 1100), 419 (479100), 399 nm (31700 $mol^{-1}dm^3cm^{-1}$); fluorescence (CH_2Cl_2, $\lambda_{exc} = 419$ nm): $\lambda_{max\,em} =$ 593, 642 nm; IR (KBr): 3433, 3044, 2967, 2956, 2922, 2856, 1750, 1728, 1600, 1522, 1478, 1439, 1367, 1328, 1267, 1206, 1177, 1150, 1067, 1028, 994, 922, 795, 750, 718, 700, 656, 467, 433 cm^{-1}; ^1H NMR (300 MHz, $CDCl_3$, 298 K): 8.97 (d, $J = 4.7$ Hz, 4H), 8.85 (d, $J = 4.7$ Hz, 4H), 8.24–8.21 (m, 8H), 7.78–7.76 (m, 10H), 5.50 (s, 4H), 4.13 (q, $J = 7.3$ Hz, 4H), 3.48 (s, 4H) 1.12 (t, $J = 7.3$ Hz, 6H); ^{13}C NMR (75.45 MHz, $CDCl_3$, 298 K): $\delta = 166.88$, 166.72, 150.59, 150.39, 143.44, 143.00, 134.67, 134.31, 133.97, 132.42, 132.16, 127.81, 127.53, 127.10, 126.82, 121.53, 120.71, 111.20, 67.43, 61.69, 41.76, 13.97; MS (FAB): *m/z* (%): 966.2 (32) $[M]^+$; MS (HR-FAB): 964.2467 $[M]^+$; calcd for $C_{56}H_{44}N_4O_8Zn$: 964.2450.

***out,out*-61,62-Diethyl 61,62-[10,20-diphenylporphyrin-5,15-diylbis(1,3-phenylene)dimethyl] 1,2:55,60-bismethano[60]fullerene-61,61,62,62-tetracarboxylate (2-) *N*^{21}, *N*^{22}, *N*^{23}, *N*^{24} *zinc* (1·Zn)**: M.p.: > 400 °C (CH_2Cl_2/hexane); UV/Vis (CH_2Cl_2): $\lambda_{max}(\varepsilon) = 586$ (3100), 548 (13200), 512 (3300), 427 (263200), 411 (sh 35400), 323 (44200), 264 nm (91200 $mol^{-1}dm^3cm^{-1}$); fluorescence (CH_2Cl_2, $\lambda_{exc} = 427$ nm): $\lambda_{max\ em} = 595$, 647 nm; IR (KBr): 2956, 2911, 2856, 1764, 1628, 1589, 1561, 1456, 1440, 1378, 1333, 1244, 1206, 1167, 1100, 1067, 1000, 794, 750, 733, 700, 527, 467 cm^{-1}; ^1H NMR (300 MHz, $CDCl_3$, 298 K): $\delta = 8.79$ (s, 8H), 8.67 (d, $J = 7$ Hz, 2H), 8.15–7.67 (m, 16H), 5.99 (s, 4H), 4.56 (q, $J = 7.1$ Hz, 4H), 1.51 (t, $J = 7.1$ Hz, 6H); ^{13}C NMR (125.8 MHz, $CDCl_3$, 298 K): $\delta = 163.66$, 163.64, 149.99, 149.74, 144.81, 144.32, 144.17, 143.39, 143.10, 142.76, 142.60, 142.53, 142.38, 141.79, 141.70, 140.79, 140.14, 139.63, 138.71, 135.53, 134.15, 134.02, 133.45, 132.24, 131.92, 131.74, 128.95, 128.14, 127.33, 126.70, 126.30, 125.42, 121.17, 119.94, 69.28, 67.90, 63.50, 45.71, 14.21; MS (HR-FAB): 1680.2143 $[M]^+$; calcd for $C_{116}H_{40}N_4O_8Zn$: 1680.2137.

61,61′-Diethyl 61,61′-[10,20-diphenylporphyrin-5,15-diylbis(1,3-phenylene)dimethyl] bis(1,2-methano[60]fullerene-61,61-dicarboxylate) (2-) *N*^{21}, *N*^{22}, *N*^{23}, *N*^{24} *zinc* (2·Zn): M.p.: > 400 °C (CH_2Cl_2/hexane); UV/Vis (CH_2Cl_2): $\lambda_{max}(\varepsilon) = 581$ (sh 3600), 550 (13300), 510 (4100), 427 (203900), 404 (sh 21600), 329 (61000), 259 nm (173000 $mol^{-1}dm^3cm^{-1}$); fluorescence (CH_2Cl_2, $\lambda_{exc} = 427$ nm): $\lambda_{max\,em} = 594$, 647 nm; IR (KBr): 2956, 2922, 2844, 1744, 1728, 1594, 1561, 1472, 1367, 1328, 1261, 1144, 1027, 1000, 967, 911, 794, 778, 733, 700, 661 cm^{-1}; ^1H NMR (300 MHz, $CDCl_3$, 298 K): $\delta = 8.85–8.82$ (m, 8H), 8.43–7.61 (m, 18H), 5.89 (s, 2H), 5.87 (s, 2H), 4.55–4.43 (m, 4H),

0947-6539/00/0609-1642 $ 17.50+.50/0 *Chem. Eur. J.* **2000**, *6*, No. 9

1.40 (t, $J = 7.1$ Hz, 3H), 1.34 (t, $J = 7.1$ Hz, 3H); ^{13}C NMR (125.8 MHz, $(CDCl_2)_2$, 298 K): $\delta = 163.63$, 163.61, 163.50, 163.46, 150.19, 150.17, 149.94, 149.91, 145.00, 144.94, 144.90, 144.84, 144.81, 144.77, 144.76, 144.73, 144.69, 144.58, 144.56, 144.47, 144.42, 144.39, 144.38, 144.35, 144.34, 144.30, 144.23, 144.16, 144.06, 143.94, 143.92, 143.61, 143.56, 143.41, 143.35, 143.33, 143.31, 143.29, 143.15, 143.14, 143.11, 143.04, 142.85, 142.81, 142.79, 142.69, 142.64, 142.61, 142.54, 142.47, 142.45, 142.41, 142.35, 142.25, 142.20, 142.05, 141.80, 141.73, 141.59, 141.53, 141.49, 141.44, 141.30, 140.83, 140.62, 140.49, 140.42, 140.06, 139.89, 139.15, 138.03, 137.82, 134.49, 133.25, 132.51, 132.12, 132.10, 132.08, 127.72, 127.70, 127.10, 126.91, 126.81, 126.80, 126.76, 126.73, 126.09, 125.32, 121.47, 121.46, 120.39, 120.38, 120.37, 71.29, 71.21, 63.87, 52.14, 14.42; MS (FAB): m/z (%): 2403.8 (82) $[M]^+$; MS (MALDI-TOF): m/z: 2403.4 $[MH]^+$; calcd for $^{13}C_2{}^{12}C_{174}H_{41}N_4O_8Zn^+$: 2403.2.

Electrochemical measurements: The measurements were performed under Ar in dry CH_2Cl_2 or benzonitrile (5 mL) containing 0.1M Bu_4NPF_6, typically using 0.5 mM solutions of the fullerene – porphyrin conjugate. An EG&G Princeton Applied Research model 263A Potentiostat/Galvanostat was used to obtain all of the measurements. A glassy carbon mini-electrode was used as the working electrode, a Ag/AgCl electrode from Bioanalytical Systems was used as the reference, and 0.5 mM Fc was added as an internal potential standard. A Pt wire served as the counter-electrode. A typical scan was run at a rate of 100 mV s^{-1}, and no solution resistance compensation was applied.

Spectroscopic and photophysical measurements: The spectroscopic investigations were carried out in toluene (Carlo Erba, spectrofluorimetric grade) and benzonitrile (Aldrich, HPLC grade). The samples were placed in fluorimetric 1 cm path cuvettes and, when necessary, purged from oxygen by bubbling Ar through. Absorption spectra were recorded with a Perkin – Elmer λ5 spectrophotometer. Uncorrected emission spectra were obtained with a Spex Fluorolog II spectrofluorimeter (continuous Xe lamp), equipped with a Hamamatsu R-928 or R-3896 (red enhanced) photomultiplier tube. The corrected spectra were obtained via a calibration curve determined by means of a 45 W quartz-halogen tungsten filament lamp (Optronic Laboratories) calibrated in the range 400 – 1800 nm. The calibration curve is flat (no correction required) between 400 and 550 nm, then increases steeply giving a correction factor of 7, 25, and 210 at 700, 800, and 850 nm, respectively. Fluorescence quantum yields obtained from spectra on an energy scale (cm^{-1}) were measured with the method described by Demas and Crosby[39] using $[Ru(bpy)_3]^{2+}$ in water ($\Phi_{em} = 0.028$)[40] or $[Os(phen)_3]^{2+}$ in acetonitrile ($\Phi_{em} = 0.005$) as standards).[41] The delayed phosphorescence spectrum of the **3·Zn** triplet was obtained with the above mentioned Spex Fluorolog II spectrometer equipped with a pulsed Xe lamp (1934D Phosphorimeter). To record the 77 K luminescence spectra, the samples were put in glass tubes (2 mm diameter) and inserted in a special quartz dewar, filled up with liquid nitrogen. When necessary, spectra of pure toluene solvent were recorded and then subtracted as background signal, in order to eliminate the contribution of the light scattered by the rigid matrix.

The steady-state IR luminescence spectra were obtained with a constructed-in-house apparatus available at the Chemistry Department of the University of Bologna (Italy) consisting of an Ar ion laser ($\lambda_{exc} = 488$ or 514 nm) that excited a sample held in a regular 1 cm path cuvette. A beam chopper (Stanford Research Systems, Inc. Model SR 540) was placed between the excitation source and the sample cuvette; luminescence was monitored at right angles to the excitation. After the light passed through suitable cut-off filters, it crossed a monochromator (Edinburgh Instruments Ltd., computer controllable) with a grating of 1200 L mm^{-1}, 1 mμ blazed. The detector was a liquid nitrogen cooled germanium detector and preamplifier (Northcoast Scientific Corp. Model EO-817L). A Northcoast muon filter (Model 829B) was used as an electronic signal filter, after the signal was sent to a lock-in amplifier (Stanford Research Systems, Inc. Model SR 510). The system was interfaced to a workstation consisting of an IBM compatible computer. The corrected IR luminescence spectra were obtained via a calibration curve determined in the same way as described for the UV/Vis spectrofluorimeter (see above). In this case, the calibration curve implies much less dramatic correction factors, 2.5 at 800 nm being the highest one.

The determination of the yields of singlet-oxygen sensitization, according to Darmanyan and Foote,[42] was obtained by monitoring the singlet-oxygen luminescence at 1270 nm and taking C_{60} in toluene as relative standard ($\Phi_D = 1.0$).[20]

Emission lifetimes on the nanosecond time scale were determined with an IBH single photon counting spectrometer equipped with a thyratron gated nitrogen lamp working at 40 kHz ($\lambda_{exc} = 337$ nm, 1 ns time resolution); the detector was a red-sensitive (185 – 850 nm) Hamamatsu R-3237-01 photomultiplier. For picosecond time resolution, an apparatus based on a single-shot streak camera (Hamamatsu C1587) and a Nd-YAG laser (PY62-10 Continuum) with a 35 ps pulse was used; a more detailed description of the system is reported elsewhere.[43] The excitation wavelength was 355 nm and the energy was 2 – 3 mJ; 2000 to 4000 laser shots were accumulated to obtain the streak images, time profiles were obtained by selecting 20 nm intervals around the emission maxima.

Transient absorption spectra and lifetimes with picosecond time resolution were obtained with a pump and probe system based on the 35 ps Nd/YAG laser (see above) and an OMA detector. Excitation with the second (532 nm) or third (355 nm) harmonic at 4 – 7 mJ of energy per pulse was used. Details on this photolysis system have been already reported.[44]

The nanosecond transient absorption spectra were recorded by using the third harmonic (355 nm) of a Nd:YAG laser (JK Lasers) with 20 ns pulse and 1 – 2 mJ of energy per pulse. The details on the flash-photolysis system are reported elsewhere.[45]

Experimental uncertainties are estimated to be $\pm 8\%$ for lifetime determination, $\pm 20\%$ for quantum yields, ± 1 nm and ± 5 nm for absorption and emission peaks, respectively.

All the experiments were performed at 298 K, unless otherwise specified.

Acknowledgement

This research was supported by the Italian National Research Council (CNR), the Swiss National Science Foundation, F. Hoffmann-La Roche, Basel, the US National Science Foundation (CHE-9313018), and a NIH Fogarty Fellowship (1F06 TW-02231-01 to L.E). We thank Prof. Alberto Juris for having allowed the use of the IR luminescence spectrometer at the Department of Chemistry of the University of Bologna (Italy), Dr. Sandra Monti and Dr. Lucia Flamigni for useful discussions, Dr. M. Sebova and S. Siefken for the ^{13}C-NMR measurements, and Dr. C. Thilgen for assistance with the nomenclature.

[1] a) P. Piotrowiak, *Chem. Soc. Rev.* **1999**, *28*, 143 – 150; b) *Molecular Electronics Devices* (Eds.: F. L. Carter, R. E. Siatowski, H. Woltjen), North Holland, Amsterdam, **1988**; c) V. Balzani, F. Scandola in *Comprehensive Supramolecular Chemistry*, *Vol. 10* (Ed.: D. N. Reinhoudt), Pergamon/Elsevier, Oxford, **1996**, pp. 687 – 746; d) M. R. Wasielewski, *Chem. Rev.* **1992**, *92*, 435 – 461; e) V. Balzani, F. Scandola, *Supramolecular Photochemistry*, Ellis Horwood, Chichester **1991**;

[2] S. I. Khan, A. M. Oliver, M. N. Paddon-Row, Y. Rubin, *J. Am. Chem. Soc.* **1993**, *115*, 4919 – 4920.

[3] a) H. Imahori, Y. Sakata, *Eur. J. Org. Chem.* **1999**, 2445 – 2457; b) F. Diederich, M. Gómez-López, *Chem. Soc. Rev.* **1999**, *28*, 263 – 277; c) T. da Ros, M. Prato, *Chem. Commun.* **1999**, 663 – 669; d) N. Martín, L. Sánchez, B. Illescas, I. Pérez, *Chem. Rev.* **1998**, 2527 – 2547; e) H. Imahori, Y. Sakata, *Adv. Mater.* **1997**, *9*, 537 – 546.

[4] a) A. Hirsch, *Top. Curr. Chem.* **1999**, *199*, 1 – 65; b) S. Samal, S. K. Sahoo, *Bull. Mat. Sci.* **1997**, *20*, 141 – 230; c) F. Diederich, C. Thilgen, *Science* **1996**, *271*, 317 – 323.

[5] a) K. A. Jolliffe, S. J. Langford, M. G. Ranasinghe, M. J. Shephard, M. N. Paddon-Row, *J. Org. Chem.* **1999**, *64*, 1238 – 1246; b) D. Kuciauskas, P. A. Liddell, S. Lin, T. E. Johnson, S. J. Weghorn, J. S. Lindsey, A. L. Moore, T. A. Moore, D. Gust, *J. Am. Chem. Soc.* **1999**, *121*, 8604 – 8614; c) X. Camps, E. Dietel, A. Hirsch, S. Pyo, L. Echegoyen, S. Hackbarth, B. Röder, *Chem. Eur. J.* **1999**, *5*, 2362 – 2373; d) P. Cheng, S. R. Wilson, D. Schuster, *Chem. Commun.* **1999**, 89 – 90; e) H. Imahori, H. Yamada, S. Ozawa, K. Ushida, Y. Sakata, *Chem. Commun.* **1999**, 1165 – 1166; f) M. Fujitsuka, O. Ito, H. Imahori, K. Yamada, H. Yamada, Y. Sakata, *Chem. Lett.* **1999**, 721 – 722; g) D. Carbonera, M. Di Valentin, C. Corvaja, G. Agostini, G. Giacometti, P. A. Liddell, D. Kuciauskas, A. L. Moore, T. A. Moore, D. Gust, *J. Am. Chem. Soc.* **1998**, *120*, 4398 – 4405; h) E. Dietel, A.

Hirsch, J. Zhou, A. Rieker, *J. Chem. Soc. Perkin Trans 2*, **1998**, 1357 – 1364; i) J.-F. Nierengarten, C. Schall, J.-F. Nicoud, *Angew. Chem.* **1998**, *110*, 2037 – 2040; *Angew. Chem. Int. Ed.* **1998**, 37, 1934 – 1936; j) J.-F. Nierengarten, L. Oswald, J.-F. Nicoud, *Chem. Commun.* **1998**, 1545 – 1546; k) S. Higashida, H. Imahori, T. Kenada, Y. Sakata, *Chem. Lett.* **1998**, 605 – 606; l) P. A. Liddell, D. Kuciauskas, J. P. Sumida, B. Nash, D. Nguyen, A. L. Moore, T. A. Moore, D. Gust, *J. Am. Chem. Soc.* **1997**, *119*, 1400 – 1405; m) P. S. Baran, R. R. Monaco, A. U. Khan, D. I. Schuster, S. R. Wilson, *J. Am. Chem. Soc.* **1997**, *119*, 8363 – 8364; n) M. G. Ranasinghe, A. M. Oliver, D. F. Rothenfluh, A. Salek, M. N. Paddon-Row, *Tetrahedron Lett.* **1996**, *37*, 4797 – 4800; o) H. Imahori, K. Hagiwara, T. Akiyama, M. Aoki, S. Taniguchi, T. Okada, M. Shirakawa, Y. Sakata, *Chem. Phys. Lett*. **1996**, *263*, 545 – 550; p) H. Imahori, Y. Sakata, *Chem. Lett*. **1996**, 199 – 200; q) T. Akiyama, H. Imahori, A. Ajawakom, Y. Sakata, *Chem. Lett.* **1996**, 907 – 908; r) D. Kuciauskas, S. Lin, G. R. Seely, A. L. Moore, T. A. Moore, D. Gust, T. Drovetskaya, C. A. Reed, P. D. W. Boyd, *J. Phys. Chem.* **1996**, *100*, 15926—15932; s) H. Imahori, K. Hagiwara, T. Akiyama, S. Taniguchi, T. Okada, Y. Sakata, *Chem. Lett.* **1995**, 265 – 266; t) T. Drovetskaya, C. A. Reed, P. Boyd, *Tetrahedron Lett*. **1995**, *36*, 7971 – 7974; u) P. Liddell, J. Sumida, A. N. Macpherson, L. Noss, G. R. Seely, K. N. Clark, A. L. Moore, T. A. Moore, D. Gust, *Photochem. Photobiol.* **1994**, *60*, 537 – 541.

[6] a) F. Diederich, R. Kessinger in *Templated Organic Synthesis* (Eds.: F. Diederich, P. J. Stang), Wiley-VCH, Weinheim, **1999**, pp. 189 – 218; b) F. Diederich, R. Kessinger, *Acc. Chem. Res.* **1999**, *32*, 537 – 545; c) J.-F. Nierengarten, V. Gramlich, F. Cardullo, F. Diederich, *Angew. Chem.* **1996**, *108*, 2242 – 2244; *Angew. Chem. Int. Ed.* **1996**, *35*, 2101 – 2103; d) L. Isaacs, R. F. Haldimann, F. Diederich, *Angew. Chem.* **1994**, *106*, 2434 – 2437; *Angew. Chem. Int. Ed.* **1994**, *33*, 2339 – 2342.

[7] For a preliminary account of parts of this work, see: J.-P. Bourgeois, F. Diederich, L. Echegoyen, J.-F. Nierengarten, *Helv. Chim. Acta* **1998**, *81*, 1835 – 1844.

[8] Staab and co-workers had previously demonstrated that the incorporation of porphyrins and quinones (as electron acceptors) into cyclophane-type dyads and triads provides enhanced control of the interchromophoric spatial relationship; see: a) H. A. Staab, S. Nikolic, C. Krieger, *Eur. J. Org. Chem.* **1999**, 1459 – 1470; b) H. A. Staab, R. Hauck, B. Popp, *Eur. J. Org. Chem.* **1998**, 631 – 642; c) H. A. Staab, B. Kratzer, S. Quazzotti, *Eur. J. Org. Chem.* **1998**, 2149 – 2160.

[9] For a macrocyclic [60]fullerene – porphyrin dyad with *trans-2* addition pattern, see: E. Dietel, A. Hirsch, E. Eichhorn, A. Rieker, S. Hackbarth, B. Röder, *Chem. Commun.* **1998**, 1981 – 1982.

[10] a) J.-P. Bourgeois, P. Seiler, M. Fibbioli, E. Pretsch, F. Diederich, *Helv. Chim. Acta* **1999**, *82*, 1572 – 1595; b) J.-P. Bourgeois, L. Echegoyen, M. Fibbioli, E. Pretsch, F. Diederich, *Angew. Chem.* **1998**, *110*, 2203 – 2207; *Angew. Chem. Int. Ed.* **1998**, *37*, 2118 – 2121.

[11] C. Bingel, *Chem. Ber.* **1993**, *126*, 1957 – 1959.

[12] Force field simulation using CVFF force field in the program Insight II 95.0 of the modeling package Discover 2. 9.7, *Biosym Technologies*, San Diego, **1997**.

[13] a) V. P. Baillargeon, J. K. Stille, *J. Am. Chem. Soc.* **1986**, *108*, 452 – 461; b) D. Tanner, O. Wennerström, *Acta. Chem. Scand. B* **1983**, *37*, 693 – 698.

[14] a) G. R. Geier, III, J. S. Lindsey, *J. Org. Chem.* **1999**, *64*, 1596 – 1603; b) B. Jiang, S.-W. Yang, D. C. Barbini, W. E. Jones Jr., *Chem. Commun.* **1998**, 213 – 214; c) F. Li, K. Yang, J. S. Tyhonas, K. A. MacCrum, J. S. Lindsey, *Tetrahedron* **1997**, *53*, 12339 – 12360; d) C.-H. Lee, J. S. Lindsey, *Tetrahedron* **1994**, *50*, 11427 – 11440; e) J. S. Manka, D. S. Lawrence, *Tetrahedron Lett.* **1989**, *30*, 6989 – 6992.

[15] a) K. Tashiro, T. Aida, J.-Y. Zheng, K. Kinbara, K. Saigo, S. Sakamoto, K. Yamaguchi, *J. Am. Chem. Soc.* **1999**, *121*, 9477 – 9478; b) D. R. Evans, N. L. P. Fackler, Z. Xie, C. E. F. Rickard, P. D. W. Boyd, C. A. Reed, *J. Am. Chem. Soc.* **1999**, *121*, 8466 – 8474; c) P. D. W. Boyd, M. C. Hodgson, C. E. F. Rickard, A. G. Oliver, L. Chaker, P. J. Brothers, R. D. Bolskar, F. S. Tham, C. A. Reed, *J. Am. Chem. Soc.* **1999**, *121*, 10487—10495; d) M. M. Olmstead, D. A. Costa, K. Maitra, B. C. Noll, S. L. Phillips, P. M. Van Calcar, A. L. Balch, *J. Am. Chem. Soc.* **1999**, *121*, 7090 – 7097; e) T. Nojiri, A. Watanabe, O. Ito, *J. Phys. Chem. A*. **1998**, *102*, 5215 – 5219.

[16] N. Armaroli, F. Diederich, L. Echegoyen, T. Habicher, L. Flamigni, G. Marconi, J.-F. Nierengarten, *New J. Chem.* **1999**, *23*, 77 – 83.

[17] a) N. Armaroli, F. Diederich, C. O. Dietrich-Buchecker, L. Flamigni, G. Marconi, J.-F. Nierengarten, J.-P. Sauvage, *Chem. Eur. J.* **1998**, *4*, 406 – 416; b) F. Diederich, U. Jonas, V. Gramlich, A. Herrmann, H. Ringsdorf, C. Thilgen, *Helv. Chim. Acta* **1993**, *76*, 2445 – 2453.

[18] a) R. W. Redmond, J. N. Gamlin, *Photochem. Photobiol.* **1999**, *70*, 391 – 475; b) F. Wilkinson, W. P. Helmann, A. B. Ross, *J. Phys. Chem. Ref. Data* **1993**, *22*, 113 – 252.

[19] a) Y.-Z. An, A. L. Viado, M.-J. Arce, Y. Rubin, *J. Org. Chem.* **1995**, *60*, 8330 – 8331; b) J. L. Anderson, Y.-Z. An, Y. Rubin, C. S. Foote, *J. Am. Chem. Soc.* **1994**, *116*, 9763 – 9764; c) J. W. Arbogast, A. O. Darmanyan, C. S. Foote, Y. Rubin, F. N. Diederich, M. M. Alvarez, S. J. Anz, R. L. Whetten, *J. Phys. Chem.* **1991**, *95*, 11 – 12.

[20] R. R. Hung, J. J. Grabowski, *J. Phys. Chem.* **1991**, *95*, 6073 – 6075.

[21] Y.-P. Sun, G. E. Lawson, J. E. Riggs, B. Ma, N. Wang, D. K. Moton, *J. Phys. Chem. A* **1998**, *102*, 5520 – 5528.

[22] a) R. Englman, J. Jortner, *Mol. Phys.* **1970**, *18*, 145 – 164. b) K. Freed, J. Jortner, *J. Chem. Phys.* **1970**, *52*, 6272 – 6291.

[23] a) W.-C. Hung, C.-D. Ho, C.-P. Liu, Y.-P. Lee, *J. Phys. Chem.* **1996**, *100*, 3927 – 3932; b) D. J. van den Heuvel, I. Y. Chan, E. J. J. Groenen, J. Schmidt, G. Meijer, *Chem. Phys. Lett.* **1994**, *231*, 111 – 118.

[24] a) F. Prat. R. Stackow, R. Bernstein, W. Qian, Y. Rubin, C. S. Foote, *J. Phys. Chem. A* **1999**, *103*, 7230 – 7235; b) K. Palewska, J. Sworakowski, H. Chojnacki, E. C. Meister, U. P. Wild, *J. Phys. Chem.* **1993**, *97*, 12167—12172.

[25] T. Hamano, K. Okuda, T. Mashino, M. Hirobe, K. Arakane, A. Ryu, S. Mashiko, T. Nagano, *Chem. Commun.* **1997**, 21 – 22.

[26] Hyperchem, Hypercube Inc., Waterloo, Canada, **1996**.

[27] S. Leach, M. Vervloet, A. Desprès, E. Bréheret, J. P. Hare, T. J. Dennis, H. W. Kroto, R. Taylor, D. R. M. Walton, *Chem. Phys.* **1992**, *160*, 451 – 466.

[28] A. Bianco, M. Maggini, G. Scorrano, C. Toniolo, G. Marconi, C. Villani, M. Prato, *J. Am. Chem. Soc.* **1996**, *118*, 4072 – 4080.

[29] a) F. D'Souza, G. R. Deviprasad, M. S. Rahman, J.-P. Choi, *Inorg. Chem.* **1999**, *38*, 2157 – 2160; b) T. Da Ros, M. Prato, D. Guldi, E. Alessio, M. Ruzzi, L. Pasimeni, *Chem. Commun.* **1999**, 635 – 636; c) J. Otsuki, K. Harada, K. Toyama, Y. Hirose, K. Araki, M. Seno, K. Takatera, T. Watanabe, *Chem. Commun.* **1998**, 1515 – 1516; d) C. A. Hunter, R. J. Shannon, *Chem. Commun.* **1996**, 1361 – 1362; e) C. A. Hunter, R. K. Hyde, *Angew. Chem.* **1996**, *108*, 2064 – 2067; *Angew. Chem. Int. Ed.* **1996**, *35*, 1936 – 1939; f) X. Chi, A. J. Guerin, R. A. Haycock, C. A. Hunter, L. D. Sarson, *J. Chem. Soc.*, *Chem. Commun.* **1995**, 2567 – 2569; g) C. A. Hunter, L. D. Sarson, *Angew. Chem.* **1994**, *106*, 2424 – 2427; *Angew. Chem. Int. Ed.* **1994**, *33*, 2313 – 2316.

[30] a) K. Tamaki, H. Imahori, Y. Nishimura, I. Yamazaki, Y. Sakata, *Chem. Commun.* **1999**, 625 – 626; b) N. V. Tkachenko, L. Rantala, A. Y. Tauber, J. Helaja, P. H. Hynninen, H. Lemmetyinen, *J. Am. Chem. Soc.* **1999**, *121*, 9378 – 9387; c) H. Imahori, K. Yamada, M. Hasegawa, S. Taniguchi, T. Okada, Y. Sakata, *Angew. Chem.* **1997**, 109, 2740 – 2742; *Angew. Chem. Int. Ed.* **1997**, *36*, 2626 – 2629; d) H. Imahori, K. Hagiwara, M. Aoki, T. Akiyama, S. Taniguchi, T. Okada, M. Shirakawa, Y. Sakata, *J. Am. Chem. Soc.* **1996**, *118*, 11771 – 11782.

[31] a) M. C. Rath, H. Pal, T. Mukherjee, *J. Phys. Chem. A* **1999**, *103*, 4993 – 5002; b) M. Fujitsuka, C. Luo, O. Ito, *J. Phys. Chem. B* **1999**, *103*, 445 – 449; c) Y. Nakamura, T. Minowa, Y. Hayashida, S. Tobita, H. Shizuka, J. Nishimura, *J. Chem. Soc. Faraday Trans.* **1996**, *92*, 377 – 382; d) Y.-P. Sun, C. E. Bunker, B. Ma, *J. Am. Chem. Soc.* **1994**, *116*, 9692 – 9699; e) Y. Wang, *J. Phys. Chem.* **1992**, *96*, 764 – 767.

[32] a) A. Osuka, S. Nakajima, T. Okada, S. Taniguchi, K. Nozaki, T. Ohno, I. Yamazaki, Y. Nishimura, N. Mataga, *Angew. Chem.* **1996**, *108*, 98 – 101; *Angew. Chem. Int. Ed.* **1996**, *35*, 92 – 95; b) T. Hayashi, T. Miyahara, S. Kumazaki, H. Ogoshi, K. Yoshihara, *Angew. Chem.* **1996**, *108*, 2096 – 2098; *Angew. Chem. Int. Ed.* **1996**, *35*, 1964 – 1966; c) A. N. Macpherson, P. A. Liddell, S. Lin, L. Noss, G. R. Seely, J. M. DeGraziano, A. L. Moore, T. A. Moore, D. Gust, *J. Am. Chem. Soc.* **1995**, *117*, 7202 – 7212.

[33] R. M. Williams, J. M. Zwier, J. W. Verhoeven, *J. Am. Chem. Soc.* **1995**, *117*, 4093 – 4099.

[34] See Ref. [1e], p. 44.

[35] P. F. Barbara, T. J. Meyer, M. A. Ratner, *J. Phys. Chem.* **1996**, *100*, 13148—13168.

0947-6539/00/0609-1644 $ 17.50+.50/0 *Chem. Eur. J.* **2000**, *6*, No. 9

[36] J. W. Verhoeven, J. Kroon, M. N. Paddon-Row; J. M. Warman in *Supramolecular Chemistry* (Eds: V. Balzani, L. De Cola), Kluwer, Dordrecht, **1992**, p. 181 – 200.
[37] G. J. Kavarnos, in *Fundamentals of Photoinduced Electron Transfer*, VCH, New York, **1993**, Ch. 6.
[38] P. Chen, T. J. Meyer, *Chem. Rev.* **1998**, *98*, 1439 – 1477.
[39] J. N. Demas, G. A. Crosby, *J. Phys. Chem.* **1971**, *75*, 991 – 1024.
[40] K. Nakamaru, *Bull. Chem. Soc. Jpn.* **1982**, *55*, 2697 – 2705.
[41] E. M. Kober, J. V. Caspar, R. S. Lumpkin, T. J. Meyer, *J. Phys. Chem.* **1986**, *90*, 3722 – 3734.
[42] A. P. Darmanyan, C. S. Foote, *J. Phys. Chem.* **1993**, *97*, 5032 – 5035.
[43] L. Flamigni, *J. Phys. Chem.* **1993**, *97*, 9566 – 9572.
[44] L. Flamigni, N. Armaroli, F. Barigelletti, V. Balzani, J.-P. Collin, J.-O. Dalbavie, V. Heitz, J.-P. Sauvage, *J. Phys. Chem. B* **1997**, *101*, 5936 – 5943.
[45] L. Flamigni, *J. Phys. Chem.* **1992**, *96*, 3331 – 3337.

Received: December 21, 1999 [F2200]